National University of Singapore

Generalized Uncertainty Principle and its Applications

Author:

Yeo Cheng Xun

Supervisor:

A/P Kuldip Singh

Co-Supervisor:

Dr. Ng Wei Khim

A thesis submitted in partial fulfilment for the degree Bachelor of Science with Honours in Physics

Department of Physics

National University of Singapore

April 6, 2014

Abstract

The Generalized Uncertainty Principle(GUP) is motivated by the predictions from the various quantum gravity theories in an attempt to unify gravity with quantum field theory. As the name suggests, GUP refers to the modified uncertainty principle which allows the quantum gravity theory predictions to be incorporated into quantum mechanics. By doing so, we see that there are effects on the usual quantum mechanical problems. In this thesis, we will be looking at the GUP algebra and how it can affect the usual quantum mechanical problems. We will show that there are new features in the deformed quantum mechanics through some examples. An example of the effects is the existence of the additional spectrum in the relativistic landau problem with minimum length(under Synder's algebra); this spectrum do not exist in the ordinary relativistic landau problem. Furthermore, in this thesis, we will be working out the relativistic landau problem under anti-Synder's algebra. We will then see that it results in a Schrodinger-like equation with a hyperbolic scarf potential, which is exactly solvable. The solutions show that an upper bound state is found to exist under such GUP with the existence of four distinct bands in the energy spectrum. It is observed that such features vanishes in the limit of $\beta \to 0$, reducing back to the original Landau problem.

Contents

Chapter 1

Introduction and Background

Generalized Uncertainty Principle(GUP), as the name suggests, is the generalization of the Heisenberg Uncertainty Principle. There are two ways to generalize the uncertainty principle: modification of the commutator definition or modification of the commutator relations: modified commutator relations(MCRs). The former refers to a modification to the left hand side of commutator relations(changing the definition of commutator), called the q-deformed quantum mechanics[1]. Such a modification leads to the commutator relations to be rewritten as

$$[X_i, P_j]_q = i\hbar\delta_{ij} \tag{1.1}$$

where $[X_i, P_j]_q = X_i P_j - qP_j X_i$. On the other hand, the latter refers to the modification to the right hand side of the commutator relations as follow

$$[X_i, P_j] = i\hbar(f(P, X)\delta_{ij} + g(X_k, P_l)) \tag{1.2}$$

[1]In this thesis, we will be focusing on the latter method. The q-deformed quantum mechanics is mentioned to provide a more detailed picture of GUP and thus, q-algebra has not been studied in this paper.

where i,j,k,l=1,2,3 and f(P,X) and $g(X_k, P_l)$ is the diagonal and off-diagonal elements of the commutator relations respectively. We will see in the following chapters (chapter 3 and 4) that by modifying the commutation relations, they will have impact on the usual quantum mechanical examples. In addition, we will show that by subjecting the functions(f(P,X) and $g(X_k, P_l)$) to constraints imposed by Jacobi identities and imposing additional constraints, which will be discussed in section 1.1.1, different classes of MCRs, corresponding to different parameters result. Before moving into the uses of these different classes of MCRs, we will first discuss on the motivation of introducing GUP and then, we will move on to the formalism and studies on deformed quantum mechanics in chapter 2, 3 and 4 respectively.

1.1 Motivation

The successful unification of the three fundamental forces(electromagnetic, strong and weak) motivated the attempt to unify gravity with quantum field theory. However, divergences in the Feynman diagrams, suggest that the theory becomes non-renormalizable. This have led to different quantum gravity theories, such as string theory, loop gravity theory and the doubly special relativity(DSR)[2], to overcome this problem. It is noteworthy that the string theory and loop gravity theory predicts an existence of minimum length while the DSR predicts the existence of a maximum momentum.

The other way to see the possible existence of a minimum length is through the distortion of spacetime. To answer the natural question of whether spacetime is made up of fundamental units leads one to ask whether there is a limit to spatial measurement precision [4]. This requires focusing large energies onto a small region of space and thus, the energy densities

[2]These theories are not the focus of this thesis and hence, are not studied in-depth but is the core to the motivation behind GUP.

cannot be neglected for its effect on the curvature of spacetime. Hence, as higher precision measurements are obtained, it will begin to diverge when the gravitational effects of the energy densities becomes significant. It is in this notion that we believe that existence of minimum length.

Putting the quantum gravity theories aside and moving back to quantum mechanics, we want to incorporate the idea of minimum length and/or maximum momentum into quantum mechanics so that we can study their effect if they do exist. It turns out that we are able to do that by first noting that minimum length is not a physical quantity but rather, it is interpreted as minimum uncertainty in position[3]. With this in mind, we will take a look at the Heisenberg uncertainty principle since it gives us information on the minimum length.

According to the Heisenberg uncertainty principle, where commutator is defined as $[X_i, P_j] = i\hbar\delta_{ij}$, the relations $\Delta x_i \Delta p_i \geq \frac{\hbar}{2}$ (for i=1,2,3) suggest that minimum length is not admissible. The Heisenberg uncertainty principle tells us that to find a minimum length, we simply allow $\Delta p_i \to \infty$, giving $\Delta x_i \to 0$. Thus, we have shown that the Heisenberg uncertainty principle does not allow for a minimum length. We would then like to consider a different uncertainty principle in the hope that it will allow for a minimum length and/or maximum momentum. To do that, we first consider a modified commutator relation[4] defined as

$$[X_i, P_j] = i\hbar(F(P)\delta_{ij} + G(P)P_iP_j). \tag{1.3}$$

Before discussing whether such a commutator relation does allow a mini-

[3]In quantum mechanics, whenever minimum length is mentioned, it is referring to minimum uncertainty in position.

[4]The MCR proposed here is one of the many MCRs. We will see that this form will result in different classes that will allow a minimum length and maximum momentum respectively.

mum length and/or maximum momentum, constraints will be imposed to obtain different classes of such modified commutator relations(MCRs) [1].

1.1.1 Classes of MCRs

Since we are modifying the right side of the commutator relation, keeping the definition of the commutator, the operators will have to fulfill the following Jacobi identities:

$$[[X_i, X_j], P_k] + [[X_j, P_k], X_i] + [[P_k, X_i], X_j] = 0 \tag{1.4}$$

$$[[P_i, P_j], X_k] + [[P_j, X_k], P_i] + [[X_k, P_i], P_j] = 0. \tag{1.5}$$

By choosing $[X_i, X_j] = [P_i, P_j] = 0$, we can easily check that the second of the Jacobi identity is trivially satisfied and the first gives the following constraints,[5]

$$G(P) = \frac{2F(P)F'(P)}{F(P) - 2F'(P)P^2} \tag{1.6}$$

where $F'(P) = \frac{dF(P)}{dP^2}$.

Further requiring that F(P) is at most quadratic[6], that is, $F(P) = 1 + \alpha_1 P + \beta_1 P^2$, where α_1 and β_1 are the deformation parameters. Two different classes are obtained by substituting F(P) into Eqn.(1.6) and Eqn.(1.3):

[5]Refer to appendix A for details of obtaining this constraint.

[6]It is the simplest form that the MCR will allow for minimum length and/or maximum momentum. Any higher order will not produce something new.

$$[X_i, P_j] = i\hbar(1-\alpha P)\left(\delta_{ij} - \alpha\frac{P_i P_j}{P}\right), \quad \text{for } \beta_1 = 0 \tag{1.7}$$

$$[X_i, P_j]_r = i\hbar[\delta_{ij} - \alpha\left(\delta_{ij}P + \frac{P_i P_j}{P}\right) + \alpha^2(\delta_{ij} r P^2 + (2r+1)P_i P_j)], \quad \text{for } \beta_1 \neq 0 \tag{1.8}$$

where the second class, the assumption $|\beta_1|P^2 << 1$ is made and relabelling $\alpha_1 = -\alpha$ and $\beta_1 = r\alpha^2$ where r is a constant.

1.1.2 1-Dimensional Subspace

Using the above classes of MCRs in 1-dimensional subspace, we will analyse the relations to see if it allows minimum length or maximum momentum. In the 1-dimensional subspace, the two classes of MCRs can be written as

$$[X, P] = i\hbar(1 - 2\alpha P + q\alpha^2 P^2) \quad \text{where q=3r+1.} \tag{1.9}$$

From the commutator relation, we can work out the uncertainty relation since $\Delta x \Delta p \geq \frac{|<[X,P]>|}{2}$. The uncertainty relation then simplifies to

$$\Delta x \geq \frac{\hbar}{2}\left(\frac{(1-\alpha < P >)^2}{\Delta p} + \frac{(q-1)\alpha^2 < P >^2}{\Delta p} + q\alpha^2 \Delta p\right). \tag{1.10}$$

The right hand side of the uncertainty relation goes to infinity when Δp goes to 0 or infinity for $q > 1$. This means that, the expression has a minimum point, leading to a minimum length Δx_{min}. Based on dimensional grounds, Δx_{min} will be of $O(\hbar\alpha)$ since α has the dimension of P^{-1}. On the other hand, if $q \leq 1$, the above MCRs do not allow a minimum length but will exhibit a maximum momentum, which will be shown in section 2.1. In addition, by plotting the above expression, the existence and non-existence of minimal length can be seen from the boundary of the allowed region. Hence, through MCRs, the ideas/predictions of the quantum theories can be incorporated into quantum mechanics.

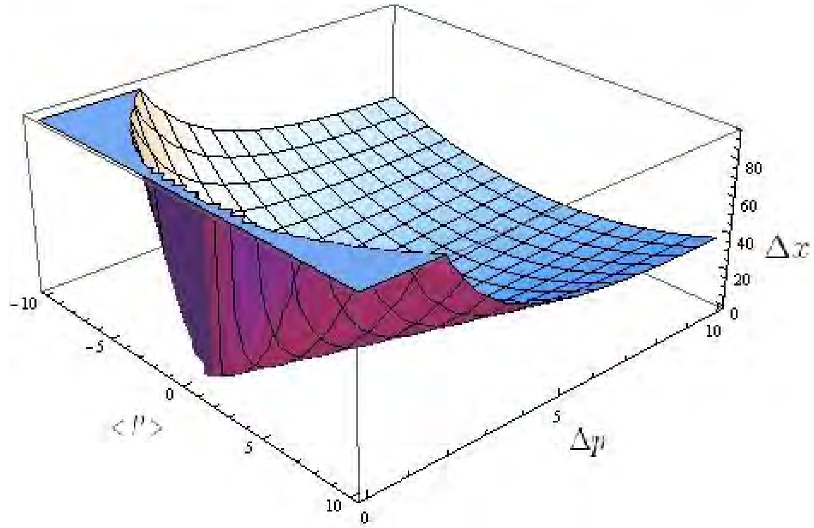

(a) q=2

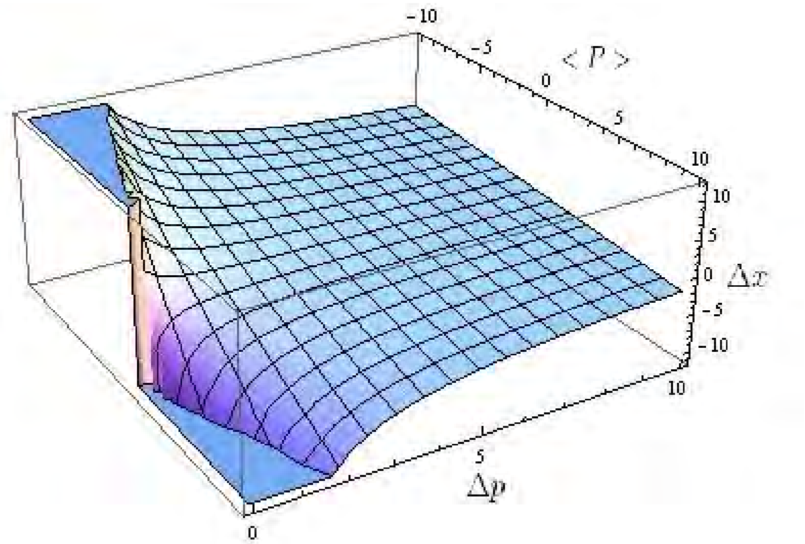

(b) q=0

Figure 1.1: A graph of boundary of the allowed region of the uncertainty relations with $\alpha = 1$ and q=2(figure 1.1a) and q=0(figure 1.1b) where the Δx is in terms of $\frac{2}{\hbar}$

1.1.3 Synder's and anti-Synder's case

From Eqn.(1.9), the Synder's[7] (and anti-Synder's) case can be obtained by assuming $\alpha \to 0$ and $q\alpha^2 \to \beta$ ($q\alpha^2 \to -\beta$) respectively. Note that β is now the deformation parameter. Taking a closer look at the Synder's case:

$$\begin{aligned} [X, P] &= i\hbar(1 + \beta P^2) \\ \Delta x \Delta p \geq& \frac{\hbar}{2}(1 + \beta(\Delta p)^2 + \beta < P >^2) \\ \frac{\hbar}{2}(\beta(\Delta p)^2 -& \frac{2}{\hbar}\Delta x \Delta p + 1 + \beta < P >^2) \leq 0. \end{aligned} \tag{1.11}$$

In order for the LHS to have real roots for Δp, it is required that

$$\frac{\Delta x}{\hbar} \geq \sqrt{\beta + (\beta < P >)^2}. \tag{1.12}$$

Therefore, the minimum length $\Delta x_{min} = \hbar\sqrt{\beta}$, which confirms the above argument that the minimum length is of $O(\hbar\alpha)$ (recall that β is of $O(\alpha^2)$).

1.2 Generalization to Higher Dimensions

Eqn.(1.7) and (1.8) are a particular class of the MCRs which allows the concept of minimum length and maximum momentum to be incorporated into quantum mechanics. They are obtained by a stringent condition that the position and momentum operator commutes among themselves. However, the result of these MCRs do not conserve rotational symmetries and hence, do not allow angular momentum.

On the other hand, the Synder's and anti-Synder's case can be gener-

[7]Synder's case is the most common MCR and is usually referred to when GUP is discussed.

alized to higher dimensions, which preserves rotational symmetries [2].

$$[X_i, P_j] = i\hbar\delta_{ij}(1 + \beta P^2) \qquad \text{(Synder)} \tag{1.13}$$

$$[X_i, P_j] = i\hbar\delta_{ij}(1 - \beta P^2) \qquad \text{(anti-Synder)} \tag{1.14}$$

It is clear that the above does indeed possess rotational symmetry. Such a rotational symmetry enables the orbital angular momentum operator to be defined as:

$$L_k = \frac{1}{1 \pm \beta P^2}\varepsilon_{ijk} X_i P_j \tag{1.15}$$

where "+" and "-" refers to Synder's and anti-Synder's case respectively. We see that the orbital angular momentum operator has a weight function $(\frac{1}{1\pm\beta P^2})$ to cancel a corresponding factor from the position operator. This is similar to the weight function introduced in the completeness relation as explained in section 2.1. While the above definitions have the usual interpretation of the angular momentum, the constraints used here in obtaining Eqn.(1.7) and (1.8) are different. It turns out that in order to fulfill the Jacobi identities, we have to relax the constraints, that is, we can only choose $[P_i, P_j] = 0$.

Hence, in these cases, the following commutation relations are obtained.

$$[P_i, P_j] = 0 \tag{1.16}$$

$$[X_i, P_j] = i\hbar\delta_{ij}(1 \pm \beta P^2) \tag{1.17}$$

$$[X_i, X_j] = \mp 2i\hbar\beta(1 \pm \beta P^2)\varepsilon_{ijk} L_k \tag{1.18}$$

$$[P_i, L_j] = i\hbar\varepsilon_{ijk} P_k \tag{1.19}$$

$$[X_i, L_j] = i\hbar\varepsilon_{ijk} X_k \tag{1.20}$$

$$[L_i, L_j] = i\hbar\varepsilon_{ijk} L_k \tag{1.21}$$

In the above, the position operators no longer commuting among themselves, which can be derived through the use of Jacobi identity[8].

[8] An example of solving for the commutator relation for the position operator is shown in section 4.1.

Chapter 2

Implications of MCRs

2.1 Hermiticity of Operators

Rewriting Eqn.(1.9) as $[X, P] = i\hbar f(P)$, in the momentum representation,

$$P = p \tag{2.1}$$

$$X = i\hbar f(p)\frac{\partial}{\partial p}. \tag{2.2}$$

Using this representation, the hermiticity of momentum operator is preserved but the hermiticity of the position operator introduces a weight function in the inner product [2]

$$< \phi|\psi >= \int \frac{dp}{f(p)}\phi^*(p)\psi(p). \tag{2.3}$$

We see that the weight function is introduced in the inner product to cancel a corresponding factor from the position operator to ensure that $< \phi|X|\psi >=< \phi|X|\psi >^*$ with the appropriate boundary conditions[9].

[9]These boundary conditions are those we used in usual quantum mechanics to prove hermiticity of an operator.

Hence, the completeness relation is then redefined as:

$$1 = \int \frac{dp}{f(p)} |p >< p|. \tag{2.4}$$

This means that the momentum eigenstates are no longer orthonormal but has a probability distribution according to the weight function,

$$< p|p' >= f(p)\delta(p - p'). \tag{2.5}$$

In Eqn.(2.3), the integrand has singularity when f(p)=0, leading to the roots $p = \frac{(1 \pm \sqrt{1-q})}{\alpha q}$, where $q \leq 1$. To avoid the singularity in the integrand, a momentum cutoff $p < p_{max}$ must be implemented, meaning that for $q \leq 1$, there is a maximum momentum cutoff.

The appearance of a maximum momentum also becomes evident when we consider the commutation relations. Recall that the constraint (Eqn.1.6), by substituting $F(P) = 1 + \alpha_1 P + \beta_1 P^2$ into the denominator, can be written as

$$G(P) = \frac{2F(P)F'(P)}{1 - \beta_1 P^2}. \tag{2.6}$$

From the above, it is observed that G(P) has a pole for $\beta_1 > 0$, implying an intrinsic maximum momentum. On the hand, when $\beta_1 < 0$, it can also introduce a maximum momentum through the weight function as discussed above.

2.2 Eigenstates of the position operator

The eigenvalue problem of the position operator in the momentum space takes the following form, for the 1-dimensional Synder's case[10]

$$i\hbar(1+\beta p^2)\partial_p\psi_\lambda(p) = \lambda\psi_\lambda(p). \tag{2.7}$$

The above differential equation can be solved to obtain the position eigenstate in momentum representation, giving

$$\psi_\lambda(p) = ke^{-i\frac{\lambda}{\hbar\sqrt{\beta}}\tan^{-1}(\sqrt{\beta}p)}. \tag{2.8}$$

However, as mentioned by Ref.[2] , the above position eigenstate is not a physical state[11]. Therefore, to obtain information on the position, it is required to study states which realize the maximally allowed localization. This refers to states with minimum length as the uncertainty in position(a 'fuzziness' in space). This means that such a state $|\psi_\xi^{ml} >$ of maximally localization around a position ξ has the following properties:

$$< \psi_\xi^{ml}|X|\psi_\xi^{ml} >= \xi \tag{2.9}$$

$$\Delta x_{|\psi_\xi^{ml}>} = \Delta x_{min}. \tag{2.10}$$

Such a state, in the momentum space, is obtained in Ref.[2] and is given by

$$\psi_\xi^{ml}(p) = \sqrt{2\frac{\sqrt{\beta}}{\pi}}(1+\beta p^2)^{1/2}e^{-i\frac{\xi\tan^{-1}(\sqrt{\beta}p)}{\hbar\sqrt{\beta}}}. \tag{2.11}$$

It is derived from deducing that such state lies on the boundary of the allowed region, that is, the boundary of the uncertainty relations $\Delta x\Delta p =$

[10]Recall that the position operator in the momentum representation is $X = i\hbar(1+\beta p^2)\frac{\partial}{\partial p}$.

[11]This state does not correspond to the observable state where it has a minimum length. Hence, it is not a physical state.

$\frac{|<[X,P]>|}{2}$. We have also seen that the minimum length occurs at $< P >= 0$ (from section 1.1.3). From the fact that such a states has the fuzziness in space, these states are no longer orthogonal as can be seen by plotting $< \psi_{\xi'}^{ml} | \psi_{\xi}^{ml} >$.

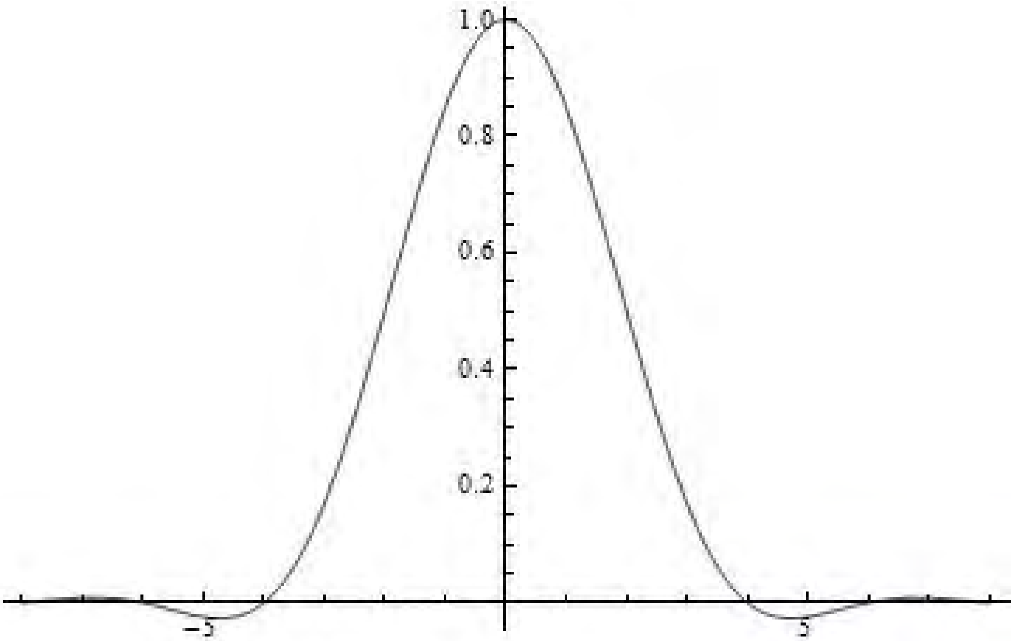

Figure 2.1: A graph of $< \psi_{\xi'}^{ml} | \psi_{\xi}^{ml} >$ plotted against $\xi - \xi'$ in units of $\hbar\sqrt{\beta}$

However, these maximally localization states are still useful in extracting information on the position of the particle. By using these maximally localization states, arbitrary states $|\phi >$ can be projected onto these states, just as in the usual quantum mechanics, to obtain the probability amplitude for the particle to be maximally localized around the position ξ. The probability of finding the particle in a region can then be calculated in the usual way.

Chapter 3

Effects of Deformed Quantum Mechanics

After understanding the changes/implications of the MCRs, we will look at the effects of the various MCRs have on the usual quantum mechanical problems. Many authors have studied the effects of deformed quantum mechanics, both non-relativistic and relativistic [1][3][5][6]. Some examples of deformed quantum mechanics that have been considered are the 1-dimensional Harmonic Oscillator, a particle in a box, the finite square well, the 1-dimensional Klein-Gordon and Dirac equations with linear confining potential and the Dirac oscillator. In the following section, several examples in these literature will be discussed to demonstrate the different effects that the various MCRs have on the usual quantum mechanics.

3.1 Non-Relativistic Quantum Mechanics

3.1.1 1-Dimensional Harmonic Oscillator

For 1-dimensional harmonic oscillator problem, the MCR in Eqn.(1.9) with q=0, will be shown in this example. Recall that q=0 case corresponds to the MCR that allows maximum momentum but no minimum length. The Schrodinger equation, in the momentum representation, is then written as,

$$\left[\frac{p^2}{(m\hbar\omega)^2} - \left(f(p)\frac{\partial}{\partial p}\right)^2\right]\Psi(p) = \frac{2E}{m(\hbar\omega)^2}\Psi(p) \tag{3.1}$$

where we have used the operators shown in section 2.1. Notice that this is not the usual differential equation we have in quantum mechanics as the second order derivative term here does not have a constant coefficient. Hence, to solve the differential equation, a change of variable from p to new variable ρ' is done ($f(p)\frac{\partial}{\partial p} \to \frac{\partial}{\partial \rho'}$, giving $p = \frac{1-e^{-2\alpha\rho'}}{2\alpha}$). The equation, with some scaling ($\rho = -2\alpha\rho'$) and in the ρ-representation, then becomes

$$\left[-\frac{\partial^2}{\partial \rho^2} + V(\rho)\right]\Psi(\rho) = \varepsilon\Psi(\rho) \tag{3.2}$$

where

$$V(\rho) = \frac{(1-e^{\rho})^2}{\delta^4}, \quad -\infty < \rho < \infty \tag{3.3}$$

and

$$\delta = 2\sqrt{m\hbar\omega}\alpha \tag{3.4}$$

$$\varepsilon = \frac{2E}{\hbar\omega\delta^2}. \tag{3.5}$$

The resulting equation is a Schrodinger-like equation where we can now solve it in the usual way. Before solving, the potential gives us some information on the bound state energies. The potential now, in contrast to the usual problem, is asymmetric since $V(\rho) \to \frac{1}{\delta^4}$ (or ∞) when $\rho \to -\infty$ (or ∞) respectively. This limits the maximum energy of the bound state spectrum, which is determined by the depth of the potential well as seen from the graph below.

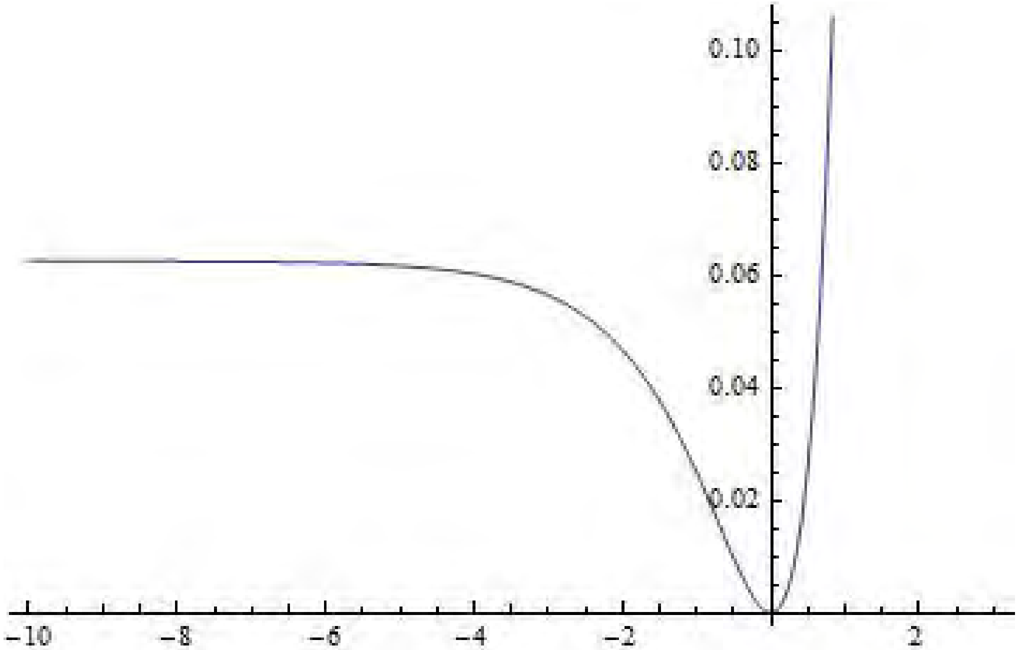

Figure 3.1: Potential of the 1-D Harmonic Oscillator with $\delta = 2$

From the graph, it is observed that although the bound state energies have a finite maximum energy, it is possible to have a continuum states of higher energies. These continuum states correspond to the scattering states just as the usual quantum mechanics would defined for states with $E > V(\rho)$ over the whole space.

Returning to the equation Eqn.(3.2), with a further change of variables,

$$\xi = \frac{2}{\delta^2} e^{\rho}; \quad 0 < \xi < \infty. \tag{3.6}$$

The resulting differential equation is given by

$$\left[\xi^2 \frac{\partial^2}{\partial \xi^2} + \xi \frac{\partial}{\partial \xi} - \frac{(1 - \frac{\delta^2}{2}\xi)^2}{\delta^4} + \epsilon \right] \Psi(\xi) = 0. \tag{3.7}$$

We can exploit the asymptotic properties to obtain an ansatz for the wavefunction [1]. Referring to appendix B, such an ansatz is obtained to be

$$\Psi(\xi) = e^{-\xi/2} f(\xi)\xi^k \tag{3.8}$$

where

$$k = \sqrt{\frac{1}{\delta^4} - \varepsilon} > 0. \tag{3.9}$$

This wavefunction will then be substituted into Eqn.(3.7) to become

$$\xi \frac{\partial^2 f(\xi)}{\partial \xi^2} + (2k + 1 - \xi) \frac{\partial f(\xi)}{\partial \xi} + \tilde{n} f(\xi) = 0 \tag{3.10}$$

where

$$\tilde{n} = \frac{1}{\delta^2}[1 - (1 - \delta^4 \varepsilon)^{1/2}] - \frac{1}{2}. \tag{3.11}$$

In order for the wavefunction to be finite when $\xi \to 0$, k is required to be positive and hence, it is easy to see from Eqn.(3.9) that

$$E_n \leq E_{max} = \frac{1}{8m\alpha^2}. \tag{3.12}$$

This is in agreement with the observation above that there is an upper bound to the energy spectrum. Writing the $f(\xi)$ as a power series, a truncation is needed to limit its growth; otherwise the wavefunction will not be normalizable at $\xi = \infty$ [1]. We see a similar truncation condition is needed in the case of the hydrogen atom. This lead to the quantization condition that $\tilde{n} = n$ where n=0, 1, 2,... Thus, the bound state energy is obtained to be

$$E_n = E_{n(0)}[1 - 2m\alpha^2 E_{n(0)}]. \tag{3.13}$$

An interesting fact, according to Ref.[1], is that the number of bound states are finite, in contrast to the usual harmonic oscillator. However, such a finite number of bound state are not found for the case when q=1 in spite of an upper bound in its energy spectrum.

Returning to Eqn.(3.10), it is observed that it has the form of a hypergeometric equation of a Laguerre polynomial[12]. Hence, the normalized wavefunctions are found to be

$$\Psi_n^{2k}(\xi) = \sqrt{\frac{4\alpha k_n n!}{\Gamma(2k_n + n + 1)}} e^{-\xi/2} \xi^{k_n} L_n^{2k_n}(\xi). \tag{3.14}$$

With the wavefunction determined explicitly, it is possible to calculate the various expectation values. It is noted that $< P > \to \frac{1}{2\alpha}$ in the limit $n \to n_{max} = \frac{1}{4m\hbar\omega\alpha^2} - \frac{1}{2}$. This is again in agreement with the q=0 theory where a maximum momentum exist.

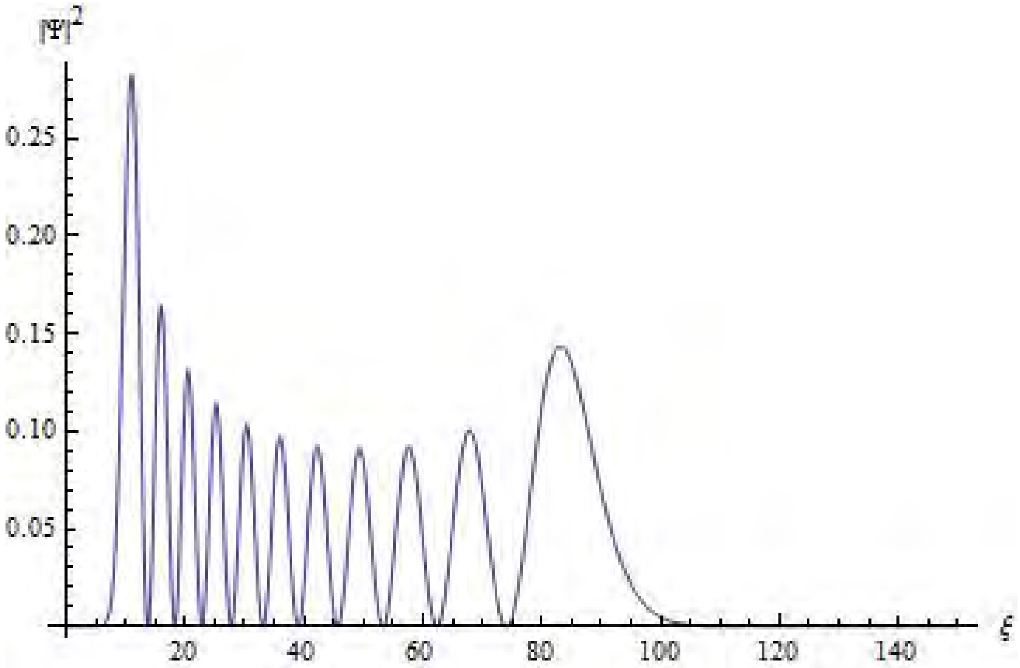

Figure 3.2: Probability density for q=0, n=10 and $\alpha = 0.1$ with $m = \hbar = \omega = 1$

From the graph above, it is evident that the probability density is asym-

[12]Explained in the appendix C.

metric, unlike the usual case. It is also worth noting that as n increases, there are more nodes and peaks but the dominant peak moves towards $\xi = 0$, meaning that there is a higher probability of finding the particle with the maximum momentum, an example is shown in the subsequent graph.

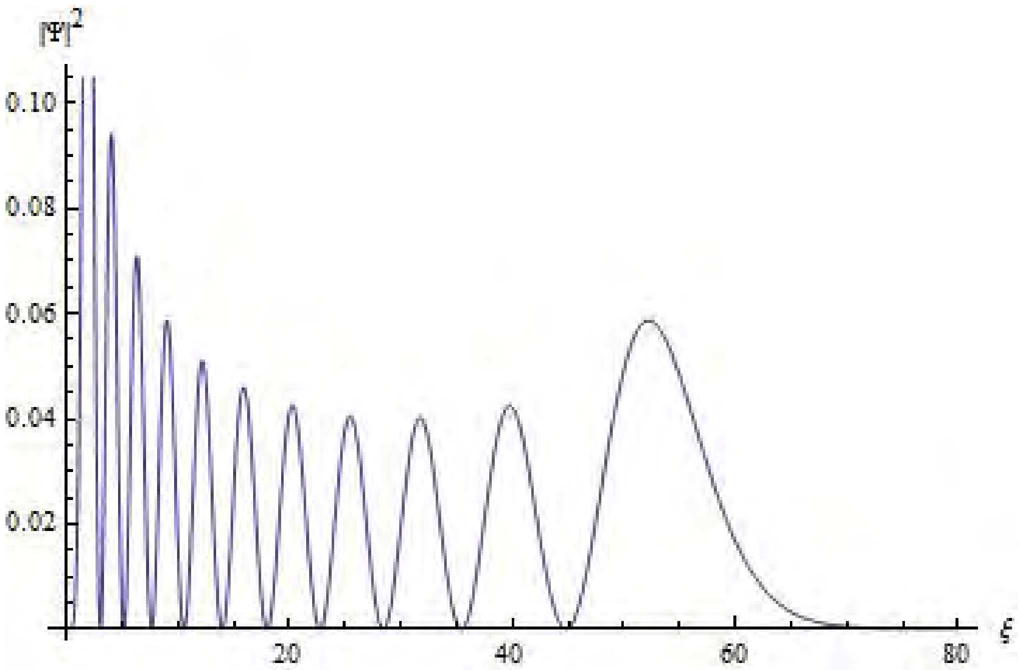

Figure 3.3: Probability density for q=0, n=20 and $\alpha = 0.1$ with $m = \hbar = \omega = 1$

This corresponds to large n bound states accumulating at the maximum momentum which results in $\Delta p = 0$ as mentioned by Ref.[1]. This can also be seen when Δp is calculated using the wavefunctions found and that it vanishes as it approaches the uppermost bound state.

3.2 Relativistic Quantum Mechanics

3.2.1 Klein-Gordon equation

Apart from looking at non-relativistic quantum mechanics, it is also interesting to investigate deformed relativistic quantum mechanics, since the particles concerned may be in the relativistic regime. In relativistic quantum mechanics, the Klein-Gordon equation can be obtained in the same way as that to Schrodinger equation [8]. The Klein-Gordon equation is used to describe spinless particles and can be written, for free particles, as

$$(P^{\mu}P_{\mu} - m^2c^2)\phi = 0 \tag{3.15}$$

where $P_{\mu} \to i\hbar\partial_{\mu}$ and in the (1+1)-dimensions, the Klein-Gordon equation is

$$\left(\frac{\partial^2}{c^2\partial t^2} - \frac{\partial^2}{\partial x^2} + \frac{m^2c^2}{\hbar^2}\right)\phi(x,t) = 0. \tag{3.16}$$

The above has a solution of a plane wave $\phi(x,t) = e^{i(kx-\omega t)}$, where $\omega = \frac{E}{\hbar}$ and $k^2 = \frac{E^2}{\hbar^2c^2} - \frac{m^2c^2}{\hbar^2}$. In the deformed case, Eqn.(1.9) will be used in the context of the Klein-Gordon equation. The q=0 case will be considered again as the effects are same for q=1 [3].

In the position representation,

$$P = f(P_0) \quad \& \quad X = X_0 \tag{3.17}$$

where P_0 and X_0 is the usual momentum and position operators satisfying Heisenberg relations. Using this definition, the exact representation can be found by solving $P = f(P_0)$ from the commutation relation, then

$$P_x = \frac{1}{2\alpha}(1 - e^{-2\alpha P_{0,x}}). \tag{3.18}$$

The Klein-Gordon equation can then be solved by noting that the solution will also be a plane wave $\phi(x,t) = e^{i(k'x-\omega t)}$, since it is a free particle. Using the same notation above, it is calculated that

$$k'_{\pm} = \frac{-ln(1 \mp 2\alpha\hbar k)}{2\alpha\hbar}. \tag{3.19}$$

Thus, the general solution is given by

$$\begin{aligned}\phi(x,t) &= e^{-i\omega t}(Ae^{\frac{-iln(1-2\alpha\hbar k)}{2\alpha\hbar}} + Be^{\frac{-iln(1+2\alpha\hbar k)}{2\alpha\hbar}}) \\ &\approx e^{-i\omega t}(Ae^{ikx(1+\alpha\hbar k)} + Be^{-ikx(1-\alpha\hbar k)}). \end{aligned} \tag{3.20}$$

In addition, an effective mass can be defined through the effective wave vectors as

$$\left(\frac{m_{\pm}c}{\hbar}\right)^2 = \frac{\omega^2}{c^2} - (k'_{\pm})^2 \tag{3.21}$$

which can be written in an expansion as

$$m_{\pm} \approx m\left[1 \mp mc\left(\frac{\hbar^2\omega^2}{m^2c^4} - 1\right)^{3/2}\alpha\right] + O(\alpha^2). \tag{3.22}$$

The above effective mass implies that the deformed Klein-Gordon equation for free particles results in the description of two particles. It is worth noting that in the limit $\alpha \to 0$, $k'_{\pm} \to \pm k$, the effective mass reduces smoothly to the ordinary mass.

3.2.2 (2+1)-Dimensional Dirac Equation In A Constant Magnetic Field

Having seen the examples of deformed quantum mechanics in presence of a maximum momentum, an example of a minimum length case will be discussed. The (2+1)-dimensional Dirac equation in an homogeneous magnetic field (relativistic Landau problem) within a minimal length scenario is studied in Ref.[6]. This example is shown for the purpose of demonstrating the effects of a minimal length for a real problem and the bounds on the deformation parameters. In addition, this problem is studied with the MCR of the Synder's case, which can be used to contrast with the focus of this project, that is, the anti-Synder's case. Since the former corresponds to the existence of minimum length and the latter corresponds a maximum momentum, the different features can be compared.

As mentioned in section 1.2, the natural generalization of the 1-dimension Synder's case is given by Eqn.(1.13), which preserves rotational symmetry. Considering (2+1)-dimensional Dirac equation in presence of a homogeneous magnetic field $\mathbf{B} = (0, 0, B_0)$, the corresponding Hamiltonian is given by

$$H = c\sigma \cdot (\mathbf{P} + \frac{e}{c}\mathbf{A}) + \sigma_z M c^2. \tag{3.23}$$

After some notations and definitions[13], the eigenvalue problem

$$H\psi = E\psi \tag{3.24}$$

can be written into the components form in two coupled equations [6]. These equations can be decoupled as:

$$P_-\psi^{(2)} = \varepsilon_-\psi^{(1)}, \quad P_+\psi^{(1)} = \varepsilon_+\psi^{(2)}, \quad \varepsilon_\pm = \frac{E \pm Mc^2}{c} \tag{3.25}$$

$$P_-P_+\psi^{(1)} = \varepsilon^2\psi^{(1)}, \quad P_+P_-\psi^{(2)} = \varepsilon^2\psi^{(2)}, \quad \varepsilon^2 = \frac{E^2 - M^2c^4}{c^2}. \tag{3.26}$$

Note that we have choosen

$$A_x = -\frac{B_0}{2}Y \quad \text{and} \quad A_y = \frac{B_0}{2}X \tag{3.27}$$

[13]The details are omitted as it is similar to the steps we will be taking in the anti-Synder's case.

and defining

$$P_{\pm} = \left(P_x + \frac{e}{c}A_x\right) \pm i\left(P_y + \frac{e}{c}A_y\right) \tag{3.28}$$

where $P_{\pm}$ are the ladder operators of the orbital angular momentum quantum number. With a further notation and writing the wavefunctions in the form[14]

$$\psi_m^{(1)} = u_m^{(1)}(p)e^{im\theta}, \qquad \psi_m^{(2)} = u_m^{(2)}(p)e^{i(m+1)\theta} \tag{3.29}$$

where m is the eigenvalue of L_z, the third component of the orbital angular momentum. Substituting the above wavefunctions, Eqn.(3.26) becomes

$$\left\{p^2 + 2\lambda(1+\beta p^2)\left[m + 1 - \beta\lambda\left(p\frac{d}{dp} - m\right)\right] - \lambda^2(1+\beta p^2)^2\left[\frac{d^2}{dp^2} + \frac{1}{p}\frac{d}{dp} - \frac{m^2}{p^2}\right]\right\}u_m^{(1)}(p) = \varepsilon^2 u_m^{(1)}(p) \tag{3.30}$$

$$\left\{p^2 + 2\lambda(1+\beta p^2)\left[m - \beta\lambda\left(p\frac{d}{dp} + m + 1\right)\right] - \lambda^2(1+\beta p^2)^2\left[\frac{d^2}{dp^2} + \frac{1}{p}\frac{d}{dp} - \frac{(m+1)^2}{p^2}\right]\right\}u_m^{(2)}(p) = \varepsilon^2 u_m^{(2)}(p). \tag{3.31}$$

The above equations can be solved by a change of variable [6]

$$u_m^{(i)}(p) = p^{-1/2}\varphi_m^{(i)}(p) \quad \text{and} \quad p = \frac{1}{\sqrt{\beta}}\tan\left(\frac{x}{2} + \frac{\pi}{4}\right), \quad x \in [-\frac{\pi}{2}, \frac{\pi}{2}] \tag{3.32}$$

[14]The form of the wavefunctions is an ansatz by considering the commutator relation $[P_{\pm}, L_z] = \mp\hbar P_{\pm}$.

to obtain a Schrodinger-like equation as shown below

$$\left\{-\frac{d^2}{dx^2}+\frac{1}{2}\left[\frac{\zeta_i(\zeta_i-1)+\xi_i(\xi_i-1)}{\cos^2(x)}\right]+\frac{1}{2}\left[\xi_i(\xi_i-1)-\zeta_i(\zeta_i-1)\right]\frac{\sin(x)}{\cos^2(x)}\right\}\varphi_m^{(i)}(x)=k^2\varphi_m^{(i)}(x) \tag{3.33}$$

where

$$k^2=\frac{\varepsilon^2+1/\beta}{4\beta\lambda^2} \tag{3.34}$$

$$\zeta_1=m+\frac{1}{2} \qquad \xi_1=m+\frac{3}{2}+\frac{1}{\beta\lambda} \tag{3.35}$$

$$\zeta_2=m+\frac{3}{2} \qquad \xi_2=m+\frac{1}{2}+\frac{1}{\beta\lambda}. \tag{3.36}$$

The above Eqn.(3.33) is a Schrodinger equation with trigonometric Scarf potential and the solution can be obtained by the hypergeometric equation or according to Ref.[6], the wavefunctions, in the momentum space, are found to be

$$u^i_{n,m}(p)=C_i\frac{p^{\zeta_i-\frac{1}{2}}}{(1+\beta p^2)^{\frac{\zeta_i+\xi_i}{2}}}*_2F_1\left(-n,\zeta_i+\xi_i+n,\zeta_i+\frac{1}{2};\frac{\beta p^2}{1+\beta p^2}\right). \tag{3.37}$$

An interesting feature is that by demanding that the wavefunctions are normalizable, the bound state spectrum consists of three regions with different ranges of the orbital angular momentum quantum number m.

$E_{n,m}=\sqrt{M^2c^4+2\hbar eB_0c(n+m)[1+\beta\frac{\hbar eB_0}{2c}(n+m)]}$, n=0,1,2,...	$\psi_{n,m}=\begin{pmatrix}\psi^1_{n,m}\\ \psi^2_{n,m}\end{pmatrix}$
$\psi^1_{n,m}(p)=C_1\frac{p^m}{(1+\beta p^2)^{m+1+\frac{1}{2\lambda\beta}}}*_2F_1\left(-n,n+2(m+1)+\frac{1}{\lambda\beta},m+1;\frac{\beta p^2}{1+\beta p^2}\right)e^{im\theta}$	
$\psi^2_{n,m}(p)=C_2\frac{p^{m+1}}{(1+\beta p^2)^{m+1+\frac{1}{2\lambda\beta}}}*_2F_1\left(-n,n+2(m+1)+\frac{1}{\lambda\beta},m+2;\frac{\beta p^2}{1+\beta p^2}\right)e^{i(m+1)\theta}$	

Table 3.1: Energy levels and the corresponding wavefunctions for $m\geq 0$. A given energy level with n+m=N has finite degeneracy D=N+1.

$E_0 = Mc^2, \quad \psi_{0,m} = \begin{pmatrix} 0 \\ \\ \psi^2_{0,m} \end{pmatrix}$	$E_n\sqrt{M^2c^4 + 2\hbar eB_0cn(1+\beta\frac{\hbar eB_0}{2c}n)}$, n=1,2,... $\quad \psi_{n,m} = \begin{pmatrix} \psi^1_{n-1,m} \\ \\ \psi^2_{n,m} \end{pmatrix}$
$\psi^1_{n,m}(p) = C_1\frac{p^{\lvert m\rvert}}{(1+\beta p^2)^{1+\frac{1}{2\lambda\beta}}} *_2 F_1\left(-n, n+2+\frac{1}{\lambda\beta}, \lvert m\rvert+1; \frac{\beta p^2}{1+\beta p^2}\right)e^{im\theta}$	
$\psi^2_{n,m}(p) = C_2\frac{p^{\lvert m+1\rvert}}{(1+\beta p^2)^{\frac{1}{2\lambda\beta}}} *_2 F_1\left(-n, n+\frac{1}{\lambda\beta}, \lvert m\rvert; \frac{\beta p^2}{1+\beta p^2}\right)e^{i(m+1)\theta}$	

Table 3.2: Energy levels and the corresponding wavefunctions for $-\frac{1}{2}-\frac{1}{\lambda\beta} < m \leq -1$. The degeneracy D of these levels is finite and explicitly given by $D = \frac{1}{2} + \frac{1}{\lambda\beta}$.

$E_{n,m} = \sqrt{M^2c^4 + 2\hbar eB_0c(n+\lvert m\rvert)[\beta\frac{\hbar eB_0}{2c}(n+\lvert m\rvert)-1]}$, n=0,1,2,...	$\psi_{n,m} = \begin{pmatrix} \psi^1_{n,m} \\ \\ \psi^2_{n,m} \end{pmatrix}$
$\psi^1_{n,m}(p) = C_1\frac{p^{\lvert m\rvert}}{(1+\beta p^2)^{\lvert m\rvert-\frac{1}{2\lambda\beta}}} *_2 F_1\left(-n, n+2\lvert m\rvert-\frac{1}{\lambda\beta}, \lvert m\rvert+1; \frac{\beta p^2}{1+\beta p^2}\right)e^{im\theta}$	
$\psi^2_{n,m}(p) = C_2\frac{p^{\lvert m\rvert-1}}{(1+\beta p^2)^{\lvert m\rvert-\frac{1}{2\lambda\beta}}} *_2 F_1\left(-n, n+2\lvert m\rvert-\frac{1}{\lambda\beta}, \lvert m\rvert; \frac{\beta p^2}{1+\beta p^2}\right)e^{i(m+1)\theta}$	

Table 3.3: Energy levels and the corresponding wavefunctions for $m < -\frac{1}{2} - \frac{1}{\lambda\beta}$. The degeneracy of the energy levels with $n + |m| = N$ and $N \geq \frac{1}{2} + \frac{1}{\lambda\beta} + 1$ is finite and given by $d = N - \frac{1}{2} - \frac{1}{\lambda\beta}$

The three regions of the bound state spectrum are shown in the above tables [6]. It is noted that in the second region, the degeneracy of the energy levels becomes infinite in the limit of a vanishing minimum length ($\beta \to 0$). On the hand, in this limit, the third region becomes meaningless since it would mean that $m < -\infty$. Thus, in this limit, this region of the spectrum vanishes. This is the interesting feature that turns out in the minimum length scenario, which is not present in the original problem. However, the physical meaning and the properties of this region has not been studied in the literature.

Moving a step further, the (2+1)-dimensional massless Dirac equation with a slight modification is applied to the graphene case. A correction term to the usual Landau levels is found to exist in the small β limit according to Ref.[6]. Also, from the energy levels calculated, the upper bound on the minimum length is obtained to be

$$\Delta x_0 = \hbar\sqrt{\beta} < 2.3nm. \tag{3.38}$$

However, this upper bound is not absolute and unique as noted in Ref.[6] as it could vary from one system to another.

Chapter 4

(2+1) dimensional Relativistic Landau problem under Anti-Synder's Algebra

We will now move onto the focus of the project where we will be working out the relativistic landau problem under anti-Synder's algebra. In this problem, we will be using the anti-Synder's case MCR. As mentioned above, the natural generalization of the anti-Synder's case in higher dimensions is given by Eqn. (1.14). Such a generalization allows for the preservation of rotational symmetry even in the the (2+1) dimensional problem as shown in the example above. Therefore, in the (2+1) dimension, the anti-Synder's case MCR[15] becomes

$$[X_i, P_j] = i\hbar\delta_{ij}(1 - \beta P^2) \quad \text{where i,j=1,2.} \tag{4.1}$$

Recall that this MCR belongs to the class which does not allow a minimum length but a maximum momentum since it has a singularity in the weight

[15] In literature, the commutation relation between spatial and temporal components are not known, hence the commutator is defined only for the spatial components.

function. In this project, we will be using the anti-Synder's algebra to study the effects of a maximum momentum on (2+1) dimensional relativistic landau problem, the same problem in the above example.

This problem, with the anti-Synder's algebra, is interesting due to the fact that the (2+1) dimensional problem has its importance in various branches of physics, especially condensed matter physics. This can be seen in the case of graphene where the Dirac equation can be modified to a massless case to describe the behaviour of the electrons in graphene. In addition, from the above examples, the deformed quantum mechanic problems present itself with different new features in presence of minimal length and maximum momentum respectively. Therefore, the (2+1) dimensional Dirac equation with the anti-Synder's algebra may present itself with new features, which it does as it is seen in the following discussions.

4.1 Background

Before moving directly into the problem, we will go through some of the background knowledge needed for this problem. The operators that satisfy Eqn.(4.1), in the momentum representation, have the following form:

$$X_i = i\hbar(1-\beta p^2)\frac{\partial}{\partial p_i} \tag{4.2}$$

$$P_i = p_i. \tag{4.3}$$

Using these representations and $[P_i, P_j] = 0$, we can work out the commutation relation $[X_i, X_j]$ from the Jacobi identity. This lead to the following equations:

$$
\begin{aligned}
&[[X_i, X_j], P_k] + [[X_j, P_k], X_i] + [[P_k, X_i], X_j] = 0 \\
&[[X_i, X_j], P_k] + i\hbar\delta_{jk}[1 - \beta P^2, X_i] - i\hbar\delta_{ik}[1 - \beta P^2, X_j] = 0 \\
&[[X_i, X_j], P_k] = i\hbar\beta\delta_{jk}(P_l[P_l, X_i] + [P_l, X_i]P_l) - i\hbar\beta\delta_{ik}(P_l[P_l, X_j] \\
&\qquad\qquad + [P_l, X_j]P_l) \\
&[[X_i, X_j], P_k] = -i\hbar\beta\delta_{jk}(2i\hbar\delta_{il}(1 - \beta P^2)P_l) + i\hbar\beta\delta_{ik}(2i\hbar\delta_{jl}(1 - \beta P^2)P_l) \\
&[[X_i, X_j], P_k] = 2\hbar^2\beta\delta_{jk}(1 - \beta P^2)P_i - 2\hbar^2\beta\delta_{ik}(1 - \beta P^2)P_j \\
&[[X_i, X_j], P_k] = 2\hbar^2\beta(1 - \beta P^2)(\delta_{jk}P_i - \delta_{ik}P_j) \\
&[[X_i, X_j], P_k] = 2\hbar^2\beta(P_iX_j - P_jX_i)P_k \\
&\implies [X_i, X_j] = 2\hbar^2\beta(P_iX_j - P_jX_i). \qquad (4.4)
\end{aligned}
$$

Hence, in the above, the position operator no longer commutes with each other; in contrast to the constraints imposed earlier to get Eqn(1.6). This is in agreement with the fact that in order to preserve rotational symmetry, we need to relax the constraint which requires the position operators to commutes.

It is interesting to note that the anti-Synder's case exhibits rotational symmetry. Hence, we are able to construct orbital angular momentum operators as defined in Eqn.(1.15) and discussed in Ref.[2]. The only orbital angular momentum operator in the (2+1) dimensional problem is

$$
L_z = \frac{1}{1 - \beta P^2}(XP_y - YP_x) = -i\hbar\partial_\theta. \qquad (4.5)
$$

Furthermore, by requiring hermiticity of the position operator, we see that the inner product between two arbitrary wavefunctions becomes

$$< \phi|\psi >= \int \frac{d^2p}{1-\beta p^2}\phi(p)\psi(p). \tag{4.6}$$

The above weight function shows that there exist a maximum momentum p_{max} where the inner product diverges and hence, to ensure normalizability, $0 < p < p_{max} = \frac{1}{\sqrt{\beta}}$ must be implemented.

4.2 The Corresponding Hamiltonian

After discussing on the background knowledge, the (2+1) dimensional Dirac equation in presence of a homogeneous magnetic field $\mathbf{B} = (0, 0, B_0)$ can be approached in the following manner. Firstly, the corresponding Hamiltonian of the Dirac equation is first written down as

$$H = c\sigma \cdot (\mathbf{P} + \frac{e}{c}\mathbf{A}) + \sigma_z Mc^2 \tag{4.7}$$

where $\sigma = (\sigma_x, \sigma_y)$ and σ_z are Pauli matrices and

$$A_x = -\frac{B_0}{2}Y \quad \text{and} \quad A_y = \frac{B_0}{2}X. \tag{4.8}$$

The eigenvalue problem is then written as

$$H\psi = E\psi \qquad \text{where} \quad \psi = \begin{pmatrix} \psi^{(1)} \\ \psi^{(2)} \end{pmatrix} \tag{4.9}$$

$$H\psi = \left[c \begin{pmatrix} 0 & P_x - iP_y \\ P_x + iP_y & 0 \end{pmatrix} + e \begin{pmatrix} 0 & A_x - iA_y \\ A_x + iA_y & 0 \end{pmatrix} + \begin{pmatrix} Mc^2 & 0 \\ 0 & Mc^2 \end{pmatrix} \right] \psi = E\psi \tag{4.10}$$

$$\begin{pmatrix} Mc^2 & P_- \\ P_+ & Mc^2 \end{pmatrix} \begin{pmatrix} \psi^{(1)} \\ \psi^{(2)} \end{pmatrix} = E \begin{pmatrix} \psi^{(1)} \\ \psi^{(2)} \end{pmatrix}. \tag{4.11}$$

Defining the ladder operators as

$$P_\pm = \left(P_x + \frac{e}{c} A_x \right) \pm i \left(P_y + \frac{e}{c} A_y \right), \tag{4.12}$$

we can then write Eqn.(4.11) into the components where they are coupled as

$$P_- \psi^{(2)} = \varepsilon_- \psi^{(1)} \tag{4.13}$$

$$P_+ \psi^{(1)} = \varepsilon_+ \psi^{(2)} \tag{4.14}$$

$$\varepsilon_\pm = \frac{E \pm Mc^2}{c}. \tag{4.15}$$

The above coupled equations can be decoupled to obtain two independent equations.

$$P_- P_+ \psi^{(1)} = \varepsilon^2 \psi^{(1)} \tag{4.16}$$

$$P_+ P_- \psi^{(2)} = \varepsilon^2 \psi^{(2)} \tag{4.17}$$

$$\varepsilon^2 = \frac{E^2 - M^2 c^4}{c^2}. \tag{4.18}$$

Defining

$$\lambda = \frac{\hbar e B_0}{2c}, \quad p_x = p\cos\theta, \quad p_y = p\sin\theta, \quad p_x^2 + p_y^2 = p^2, \tag{4.19}$$

the ladder operators in the momentum representation can be written as

$$P_\pm = pe^{\pm i\theta} - \lambda(1-\beta p^2)\left[\pm\frac{\partial}{\partial p_x} + i\frac{\partial}{\partial p_y}\right]$$

$$P_\pm = pe^{\pm i\theta} - \lambda(1-\beta p^2)\left[\pm\left(\frac{p\cos\theta}{p}\frac{\partial}{\partial p} \; - \frac{p\sin\theta}{p^2}\frac{\partial}{\partial\theta}\right) + i\left(\frac{p\sin\theta}{p}\frac{\partial}{\partial p} + \frac{\cos\theta}{p}\frac{\partial}{\partial\theta}\right)\right]$$

$$P_\pm = e^{\pm i\theta}\left[p - \lambda(1-\beta p^2)\left[\pm\frac{\partial}{\partial p} + \frac{i}{p}\frac{\partial}{\partial\theta}\right]\right]. \tag{4.20}$$

Using Eqn.(4.20), we find that $[P_\pm, L_z] = \mp\hbar P_\pm$ because $L_z = -i\hbar\frac{\partial}{\partial\theta}$, defined in the usual way. This confirms that $P_\pm$ is indeed a ladder operator and from $[P_\pm, L_z] = \mp\hbar P_\pm$, one can introduce the ansatz,

$$\psi_m^{(1)} = u_m^{(1)}(p)e^{im\theta} \tag{4.21}$$

$$\psi_m^{(2)} = u_m^{(2)}(p)e^{i(m+1)\theta} \tag{4.22}$$

where m is the eigenvalue of L_z, the third component of orbital angular momentum. Using the above ansatz, the decoupled equations, in momentum representation, are

$$
\begin{aligned}
& P_{\mp}P_{\pm}\psi_m^{(j)} \\
=& P_{\mp}P_{\pm}u_m^{(j)}(p)e^{im'_j\theta} \\
=& P_{\mp}\left(e^{\pm i\theta}\left[p\psi_m^{(j)}(p)-\lambda(1-\beta p^2)\left[\pm e^{im'_j\theta}\frac{\partial}{\partial p}u_m^{(j)}(p)-\frac{m'_j}{p}\psi_m^{(j)}(p)\right]\right]\right) \\
=& e^{\mp i\theta}\left[p-\lambda(1-\beta p^2)\left[\mp\frac{\partial}{\partial p}+\frac{i}{p}\frac{\partial}{\partial\theta}\right]\right] \\
& \left(e^{\pm i\theta}\left[p\psi_m^{(j)}(p)-\lambda(1-\beta p^2)\left[\pm e^{im'_j\theta}\frac{\partial}{\partial p}u_m^{(j)}(p)-\frac{m'_j}{p}\psi_m^{(j)}(p)\right]\right]\right) \\
=& \varepsilon^2\psi_m^{(j)}(p), \qquad \text{where } m'_j\text{=m or m+1 for j=1 or 2 respectively.}
\end{aligned}
$$

After simplifying the above, it reduces to

$$
\left[p^2+2\lambda(1-\beta p^2)\left[m'_j\pm 1+\lambda\beta\left(p\frac{\partial}{\partial p}\mp m'_j\right)\right]-\lambda^2(1-\beta p^2)^2\left[\frac{\partial^2}{\partial p^2}+\frac{1}{p}\frac{\partial}{\partial p}-\frac{m'^2_j}{p^2}\right]\right]u_m^{(j)}(p)=\varepsilon^2u_m^{(j)}(p). \tag{4.23}
$$

4.3 Solution to the problem

To solve the above equation, we will do a change of variable in two steps to simplify the equation: firstly, $u_m^{(j)}=p^{-1/2}\varphi_m^{(j)}$,

$$
\begin{aligned}
&\left[p^2+2\lambda(1-\beta p^2)\left[m'_j\pm 1+\lambda\beta\left(p\frac{\partial}{\partial p}\mp m'_j-\frac{1}{2}\right)\right]\right. \\
&\left.-\lambda^2(1-\beta p^2)^2\left[\frac{\partial^2}{\partial p^2}+\frac{1}{p^2}\left(\frac{1}{4}-m'^2_j\right)\right]\right]\varphi_m^{(j)}(p)=\varepsilon^2\varphi_m^{(j)}(p).
\end{aligned} \tag{4.24}
$$

With this simplified equation, it can be further cast into Schrodinger-like equation with another change of variable[16] as follows:

$$p = \frac{\tanh q}{\sqrt{\beta}}, \qquad q \in [0, \infty). \tag{4.25}$$

The above equation ensures that $0 < p < 1/\sqrt{\beta}$ since $\tanh q \to 1$ when $q \to \infty$. Hence, with this change of variable, the above equation, in the q-domain, becomes

$$\begin{aligned}\Bigg[-\lambda^2\beta\frac{d^2}{dq^2} + \frac{2\lambda}{\cosh^2 q}\left[(m'_j \pm 1) + \lambda\beta(\mp m'_j - \frac{1}{2})\right] + \frac{\tanh^2 q}{\beta} \\ - \frac{\lambda^2\beta}{\sinh^2 q\cosh^2 q}\left(\frac{1}{4} - m'^2_j\right)\Bigg]\varphi^{(j)}_m(q) = \varepsilon^2\varphi^{(j)}_m(q).\end{aligned} \tag{4.26}$$

This is the Schrodinger-like equation that we are familiar with. On closer examination, the Schrodinger-like equation has a potential, which consists of hyperbolic functions. This suggests that the equation may be exactly solvable if it reduces to the hyperbolic scarf potential $V_h^{(a,b)}(x)$ (Eqn.(4.34)). In order to do that, we need to represent the radial momentum in a complex plane through the following transformation

$$p = \frac{\tanh q}{\sqrt{\beta}} \to p' = \frac{\tanh(\frac{1}{2}x + i\frac{\pi}{4})}{\sqrt{\beta}} \tag{4.27}$$

where

$$p = Re[p'] \quad \text{and} \quad x \in [0, \infty). \tag{4.28}$$

With this transformation, Eqn.(4.26), in the x-domain[17], reduces to

[16] The choice of variable results from demanding that the resulting equation do not contain first order derivative. It can be found by letting $p = \frac{f(q)}{\sqrt{\beta}}$ then setting the coefficient of the first order derivative to zero.

[17] The variable x here is just another variable and should not to be confused with position eigenvalues.

$$\left[-\frac{d^2}{dx^2} + \mu sech^2 x + \nu sechx \tanh x\right] \varphi_m^{(j)} = k^2 \varphi_m^{(j)} \tag{4.29}$$

where

$$\mu = \frac{1}{\beta\lambda}(m'_j \pm 1 + \lambda\beta(\mp m'_j - \frac{1}{2})) + \frac{1}{4} - m'^2_j - \frac{1}{2\beta^2\lambda^2} \tag{4.30}$$

$$\nu = \frac{i}{2\beta^2\lambda^2} - \frac{i}{\beta\lambda}(m'_j \pm 1 + \lambda\beta(\mp m'_j - \frac{1}{2})) \tag{4.31}$$

$$k^2 = \frac{\varepsilon^2 - 1/\beta}{4\beta\lambda^2}. \tag{4.32}$$

Before proceeding further, it is interesting to note that in the x-domain, the wavefunction can also exist in the negative region. Taking into account of the range of the radial momentum p, the following transformation and change of variables yield the same equation as Eqn.(4.29)

$$p = -\frac{\tanh q}{\sqrt{\beta}} \to p' = -\frac{\tanh(\frac{1}{2}x + i\frac{\pi}{4})}{\sqrt{\beta}}, \qquad x \in (-\infty, 0]. \tag{4.33}$$

Thus, in the x-domain, the potential in Eqn.(4.29) reduces to the form of $V_h^{(a,b)}$, in which Eqn.(4.29) is exactly solvable [7]. Now,

$$V_h^{(a,b)}(x) = a^2 + (b^2 - a^2 - a\alpha) sech^2(\alpha x) + b(2a + \alpha) sech(\alpha x) \tanh(\alpha x) \tag{4.34}$$

where in the case of $\alpha = 1$, we can identify

$$b^2 - a^2 - a = \mu = \frac{1}{\beta\lambda}(m'_j \pm 1 + \lambda\beta(\mp m'_j - \frac{1}{2})) + \frac{1}{4} - m'^2_j + \frac{1}{2\beta^2\lambda^2} \tag{4.35}$$

$$b(2a + 1) = \nu = -\frac{i}{2\beta^2\lambda^2} - \frac{i}{\beta\lambda}(m'_j \pm 1 + \lambda\beta(\mp m'_j - \frac{1}{2})). \tag{4.36}$$

Eqn.(4.29) can be further reduced to a hypergeometric equation, which is exactly the differential equation satisfied by Romanovski polynomials

$R_n^{(a+\frac{1}{2},-2b)}(z)$. $R_n^{(a+\frac{1}{2},-2b)}(z)$ can be constructed through the Rodrigues representation as mentioned in appendix C. Hence, the solution of the equation is given by

$$\varphi_{m,n}^{(j)}(x) = (\sinh^2 x + 1)^{-\frac{a_j}{2}} e^{-b_j \tan^{-1}(\sinh x)} R_n^{(a_j+\frac{1}{2},-2b_j)}(\sinh x) \tag{4.37}$$

with

$$k^2 = -(a_j - n)^2$$
$$E^2 = M^2c^4 + c^2\left(\frac{1}{\beta} - 4\beta\lambda^2(a_j - n)^2\right) \tag{4.38}$$

where a_j and b_j are the parameters of the Romanovski polynomials. These are solved[18] through the simultaneous equations (4.35) and (4.36) with n being the order of the polynomial(i.e., n=0,1,2,...). After solving them, we obtain

for j=1, the four solutions are

$$a_1 = -\frac{1}{2\beta\lambda}, \qquad b_1 = \frac{i}{2}\left(1 + 2m - \frac{1}{\beta\lambda}\right) \tag{4.39}$$
$$a_1 = \frac{1}{2}\left(2m - \frac{1}{\beta\lambda}\right), \qquad b_1 = \frac{i}{2}\left(1 - \frac{1}{\beta\lambda}\right) \tag{4.40}$$
$$a_1 = \frac{1}{2}\left(-2 - 2m + \frac{1}{\beta\lambda}\right), \qquad b_1 = \frac{i}{2}\left(-1 + \frac{1}{\beta\lambda}\right) \tag{4.41}$$
$$a_1 = \frac{1}{2}\left(-2 + \frac{1}{\beta\lambda}\right), \qquad b_1 = \frac{i}{2}\left(-1 - 2m + \frac{1}{\beta\lambda}\right) \tag{4.42}$$

[18] b is set to be complex.

while for j=2,

$$a_2 = \frac{1}{2\beta\lambda}, \qquad b_2 = \frac{i}{2}\left(-1 - 2m + \frac{1}{\beta\lambda}\right) \tag{4.43}$$

$$a_2 = \frac{1}{2}\left(2m - \frac{1}{\beta\lambda}\right), \qquad b_2 = \frac{i}{2}\left(-1 - \frac{1}{\beta\lambda}\right) \tag{4.44}$$

$$a_2 = \frac{1}{2}\left(-2 - 2m + \frac{1}{\beta\lambda}\right), \qquad b_2 = \frac{i}{2}\left(1 + \frac{1}{\beta\lambda}\right) \tag{4.45}$$

$$a_2 = \frac{1}{2}\left(-2 - \frac{1}{\beta\lambda}\right), \qquad b_2 = \frac{i}{2}\left(1 + 2m - \frac{1}{\beta\lambda}\right). \tag{4.46}$$

The above values of a_j are subjected to bounds imposed by the finite orthogonality property of the Romanovski polynomials. As mentioned by Ref.[7], the polynomials have orthogonal properties with respect to their weight functions as long as weight function decreases as x^{-2a-1}. Also integral of the type

$$\int_{-\infty}^{\infty} (z^2+1)^{-(a+\frac{1}{2})} e^{-2b\tan^{-1} z} R_n^{(a+\frac{1}{2},-2b)}(z) R_{n'}^{(a+\frac{1}{2},-2b)}(z) dz \tag{4.47}$$

will be convergent only if

$$n + n' < 2(a + \frac{1}{2}) - 1 = 2a. \tag{4.48}$$

From the orthogonality property of the Romanovski polynomials, there is a finite number of bound states determined by the inequality, where the uppermost bound state n is bounded by the value of a_j, which is $n_{max} < a_j$.

Furthermore, in order for the weight function to decrease as x^{-2a-1}, it is required that $2a + 1 > 0$. In addition, from Eqn.(4.38), $E^2 \geq M^2c^4$, we then have

$$\frac{1}{\beta} - 4\beta\lambda^2(a_j - n)^2 \geq 0. \tag{4.49}$$

When n=0, we obtain a constraint on a_j,

$$\frac{1}{\beta} - 4\beta\lambda^2 a_j^2 \geq 0$$
$$a_j \leq \frac{1}{2\beta\lambda}. \tag{4.50}$$

Thus, to satisfy $-\frac{1}{2} < a_j \leq \frac{1}{2\beta\lambda}$, we obtain the following energy spectrum by solving for the ranges of m values (see Eqns.(4.39) to (4.42) and Eqns.(4.43) to (4.46)). The corresponding negative energy eigenvalues can be obtained through Eqn.(4.38). The energy spectrum and states are arranged according to the orbital angular momentum quantum number m and building the spinors with same energy eigenvalues.

$E_{m,n} = \sqrt{M^2c^4 + c^2\left(\frac{1}{\beta} - 4\beta\lambda^2(m - \frac{1}{2\beta\lambda} - n)^2\right)}$,		$n = 0, 1, 2, ... < a_j$
$\psi_{m,n}(p) = \begin{pmatrix} \psi^{(1)}_{m,n}(p) \\ \psi^{(2)}_{m,n}(p) \end{pmatrix}$	$\psi^{(1)}_{m,n}(p) = p^{-\frac{1}{2}}(\frac{1}{1-\beta p^2})^{-\frac{a_1}{2}} e^{-b_1 \tan^{-1}\left(\frac{\sqrt{\beta}p}{\sqrt{1-\beta p^2}}\right)} R_n^{(a_1+\frac{1}{2}, -2b_1)}(\frac{\sqrt{\beta}p}{\sqrt{1-\beta p^2}}) e^{im\theta}$,	
	$a_1 = m - \frac{1}{2\beta\lambda}$,	$b_1 = \frac{i}{2}\left(1 - \frac{1}{\beta\lambda}\right)$
	$\psi^{(2)}_{m,n}(p) = p^{-\frac{1}{2}}(\frac{1}{1-\beta p^2})^{-\frac{a_2}{2}} e^{-b_2 \tan^{-1}\left(\frac{\sqrt{\beta}p}{\sqrt{1-\beta p^2}}\right)} R_n^{(a_2+\frac{1}{2}, -2b_2)}(\frac{\sqrt{\beta}p}{\sqrt{1-\beta p^2}}) e^{i(m+1)\theta}$,	
	$a_2 = m - \frac{1}{2\beta\lambda}$,	$b_2 = \frac{i}{2}\left(-1 - \frac{1}{\beta\lambda}\right)$

Table 4.1: Energy levels and the corresponding wavefunctions for $-\frac{1}{2} + \frac{1}{2\beta\lambda} < m \leq \frac{1}{\beta\lambda}$.

$E_{m,n} = \sqrt{M^2c^4 + c^2\left(\frac{1}{\beta} - 4\beta\lambda^2(-1 - m + \frac{1}{2\beta\lambda} - n)^2\right)}$,		$n = 0, 1, 2, ... < a_j$
$\psi_{m,n}(p) = \begin{pmatrix} \psi^{(1)}_{m,n}(p) \\ \psi^{(2)}_{m,n}(p) \end{pmatrix}$	$\psi^{(1)}_{m,n}(p) = p^{-\frac{1}{2}}(\frac{1}{1-\beta p^2})^{-\frac{a_1}{2}} e^{-b_1 \tan^{-1}\left(\frac{\sqrt{\beta}p}{\sqrt{1-\beta p^2}}\right)} R_n^{(a_1+\frac{1}{2}, -2b_1)}(\frac{\sqrt{\beta}p}{\sqrt{1-\beta p^2}}) e^{im\theta}$,	
	$a_1 = -1 - m + \frac{1}{2\beta\lambda}$,	$b_1 = \frac{i}{2}\left(-1 + \frac{1}{\beta\lambda}\right)$
	$\psi^{(2)}_{m,n}(p) = p^{-\frac{1}{2}}(\frac{1}{1-\beta p^2})^{-\frac{a_2}{2}} e^{-b_2 \tan^{-1}\left(\frac{\sqrt{\beta}p}{\sqrt{1-\beta p^2}}\right)} R_n^{(a_2+\frac{1}{2}, -2b_2)}(\frac{\sqrt{\beta}p}{\sqrt{1-\beta p^2}}) e^{i(m+1)\theta}$,	
	$a_2 = -1 - m + \frac{1}{2\beta\lambda}$,	$b_2 = \frac{i}{2}\left(1 + \frac{1}{\beta\lambda}\right)$

Table 4.2: Energy levels and the corresponding wavefunctions for $-1 \leq m < \frac{1}{2\beta\lambda} - \frac{1}{2}$.

$E_{m,n} = \sqrt{M^2c^4 + c^2\left(\frac{1}{\beta} - 4\beta\lambda^2(\frac{1}{2\beta\lambda} - n)^2\right)}$,		$n = 1, 2, ... < \frac{1}{2\beta\lambda}$ for $\frac{1}{\beta\lambda} > 1$
$\psi_{m,n}(p) = \begin{pmatrix} \psi^{(1)}_{m,n-1}(p) \\ \psi^{(2)}_{m,n}(p) \end{pmatrix}$	$\psi^{(1)}_{m,n-1}(p) = p^{-\frac{1}{2}}(\frac{1}{1-\beta p^2})^{-\frac{a_1}{2}} e^{-b_1 \tan^{-1}\left(\frac{\sqrt{\beta}p}{\sqrt{1-\beta p^2}}\right)} R_{n-1}^{(a_1+\frac{1}{2},-2b_1)}(\frac{\sqrt{\beta}p}{\sqrt{1-\beta p^2}}) e^{im\theta}$,	
	$a_1 = -1 + \frac{1}{2\beta\lambda}$,	$b_1 = \frac{i}{2}\left(-1 - 2m + \frac{1}{\beta\lambda}\right)$
	$\psi^{(2)}_{m,n}(p) = p^{-\frac{1}{2}}(\frac{1}{1-\beta p^2})^{-\frac{a_2}{2}} e^{-b_2 \tan^{-1}\left(\frac{\sqrt{\beta}p}{\sqrt{1-\beta p^2}}\right)} R_{n}^{(a_2+\frac{1}{2},-2b_2)}(\frac{\sqrt{\beta}p}{\sqrt{1-\beta p^2}}) e^{i(m+1)\theta}$,	
	$a_2 = \frac{1}{2\beta\lambda}$,	$b_2 = \frac{i}{2}\left(-1 - 2m + \frac{1}{\beta\lambda}\right)$
$E_{m,0} = Mc^2$	, n=0,	for $\frac{1}{\beta\lambda} > 1$
$\psi_{m,0}(p) = \begin{pmatrix} 0 \\ \psi^{(2)}_{m,0}(p) \end{pmatrix}$	$\psi^{(2)}_{m,0}(p) = p^{-\frac{1}{2}}(\frac{1}{1-\beta p^2})^{-\frac{a_2}{2}} e^{-b_2 \tan^{-1}\left(\frac{\sqrt{\beta}p}{\sqrt{1-\beta p^2}}\right)} R_{0}^{(a_2+\frac{1}{2},-2b_2)}(\frac{\sqrt{\beta}p}{\sqrt{1-\beta p^2}}) e^{i(m+1)\theta}$,	
	$a_2 = \frac{1}{2\beta\lambda}$,	$b_2 = \frac{i}{2}\left(-1 - 2m + \frac{1}{\beta\lambda}\right)$
$E_{m,n} = \sqrt{M^2c^4 + c^2\left(\frac{1}{\beta} - 4\beta\lambda^2(a_2 - n)^2\right)}$,		$n = 0, 1, 2, ... < \frac{1}{2\beta\lambda}$ for $\frac{1}{\beta\lambda} \leq 1$
$\psi_{m,n}(p) = \begin{pmatrix} 0 \\ \psi^{(2)}_{m,n}(p) \end{pmatrix}$	$\psi^{(2)}_{m,n}(p) = p^{-\frac{1}{2}}(\frac{1}{1-\beta p^2})^{-\frac{a_2}{2}} e^{-b_2 \tan^{-1}\left(\frac{\sqrt{\beta}p}{\sqrt{1-\beta p^2}}\right)} R_{n}^{(a_2+\frac{1}{2},-2b_2)}(\frac{\sqrt{\beta}p}{\sqrt{1-\beta p^2}}) e^{i(m+1)\theta}$,	
	$a_2 = \frac{1}{2\beta\lambda}$,	$b_2 = \frac{i}{2}\left(-1 - 2m + \frac{1}{\beta\lambda}\right)$

Table 4.3: Energy levels independent of m and the corresponding wavefunctions for $m < -1$, $m > \frac{1}{\beta\lambda}$.

4.4 Results and Discussions

From Eqns.(4.35) and (4.36) and the various boundaries on the values of a_j, we realize that one of the solutions for the value a_j for both components cannot satisfy the boundaries and thus, is not part of the solutions. The last solution offer energy levels that are independent of the orbital angular momentum m as shown in table 4.3.

The tables above show that, under the anti-Synder's algebra, the energy spectrum results in four distinct bands in contrast to the usual case. Three out of the four bands are dependent on the value of the deformation parameter β, that is, the range of values of m in each band varies with β. In the limit of $\beta \to 0$, the states in table 4.1 vanishes as the range of m becomes meaningless. Furthermore, many of the states in table 4.3 vanishes for the same reason, leaving only the states with $m < -1$. Hence, in the limit, $\beta \to 0$, the energy spectrum reduces to two distinct bands as would be expected in the undeformed case(as discussed later).

On the other hand, a finite value of β, places an upper bound to the bound states. As seen from the orthogonality properties of Romanovski polynomials, the uppermost bound state $n_{max} < a_j$ is dependent on the value of a_j, which is in turn dependent on β. This can be seen as an upper bound on the momentum(maximum momentum) since total relativistic energy depends on momentum for a constant mass, an upper bound on the energy implies a finite maximum momentum. In the limit of $\beta \to 0$, it is noted that the number of bound states becomes infinite, and this reduces to the undeformed case.

In table 4.3, it is noted that there are two different scenario. Firstly, for $\frac{1}{\beta\lambda} > 1$, interestingly, the ground state is a spin singlet while the excited states are spin doublets. This is similar to the observation made with the Synder's algebra. In contrast, for $\frac{1}{\beta\lambda} \leq 1$, the states are all spin singlets.

Next, we will take a look on how the wavefunctions behave as n increases. The probability density is

$$
\begin{aligned}
< \psi|\psi > &= N^2 \int \frac{d^2\mathbf{p}}{1-\beta p^2} \left(\psi^{(1)*}_{m,n}(p)\psi^{(1)}_{m,n}(p) + \psi^{(2)*}_{m,n}(p)\psi^{(2)}_{m,n}(p)\right) \\
&= N'^2 \int_0^{\frac{1}{\sqrt{\beta}}} \frac{pdp}{1-\beta p^2} \left(u^{(1)*}_{m,n}(p)u^{(1)}_{m,n}(p) + u^{(2)*}_{m,n}(p)u^{(2)}_{m,n}(p)\right)
\end{aligned}
$$

$$
< \psi|\psi >= N'^2 \int_0^{\frac{1}{\sqrt{\beta}}} \frac{dp}{1-\beta p^2} \left(\varphi^{(1)*}_{m,n}(p)\varphi^{(1)}_{m,n}(p) + \varphi^{(2)*}_{m,n}(p)\varphi^{(2)}_{m,n}(p)\right) \quad (4.51)
$$

where N is the normalizing constant and $N'^2 = 2\pi N^2$. Furthermore, the probability density in the x-domain is given by

$$
< \psi|\psi >= N"^2 \int_{-\infty}^{\infty} dx \left(\varphi^{(1)*}_{m,n}(x)\varphi^{(1)}_{m,n}(x) + \varphi^{(2)*}_{m,n}(x)\varphi^{(2)}_{m,n}(x)\right). \quad (4.52)
$$

In the x-domain, we see that the probability density is symmetrical about x=0. It is noted that for both states(n=2 and n=20), the probability densities peak at x=0 where it corresponds to p=0 and vanishes at $x = \infty(-\infty)$ corresponding to $p = \frac{1}{\sqrt{\beta}}$. Furthermore, there is a widening of the peak and a reduction in the peak height as n increases. This means that as n increases, there is a decreasing probability of finding the particle with p=0 but we have a wider distribution of momentum. However, it is observed that this is a gradual change as portrayed in the graph, comparing probability density of the nth state with an order difference.

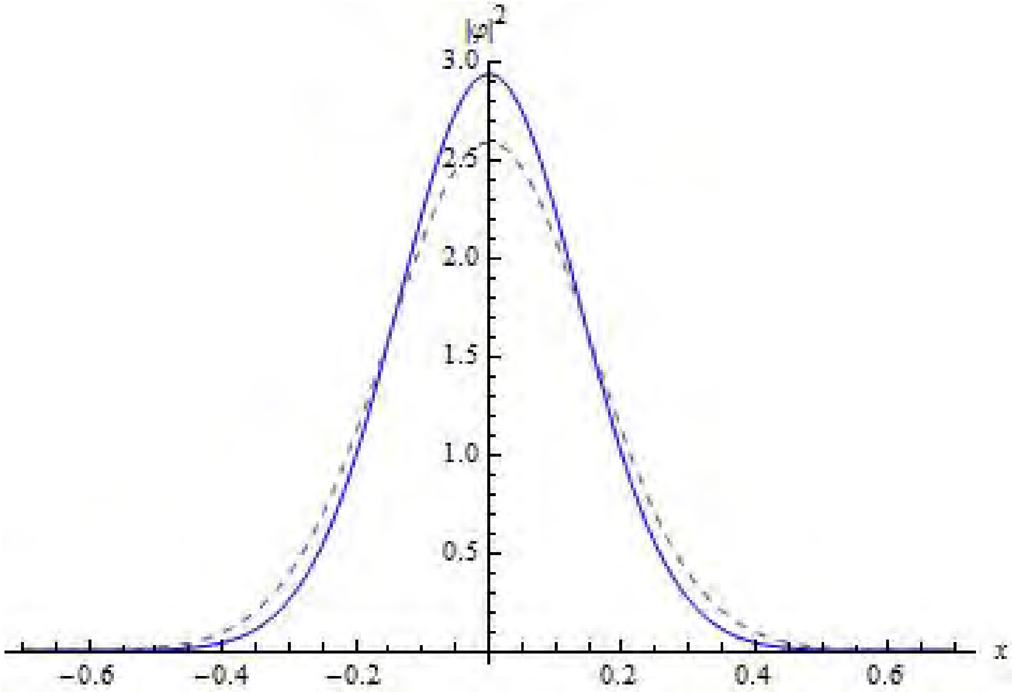

Figure 4.1: Probability density in the x-domain for $\frac{1}{2\beta\lambda} = 30$ and m=59 for n=2(solid line) and n=20(dotted line)

The probability density in the momentum space is also plotted to show that the information in the x-domain can be transported back into the momentum space as shown in the graph below. It is observed that the probability density in the momentum space has the same gradual widening and reduction in the peak height as the n increases.

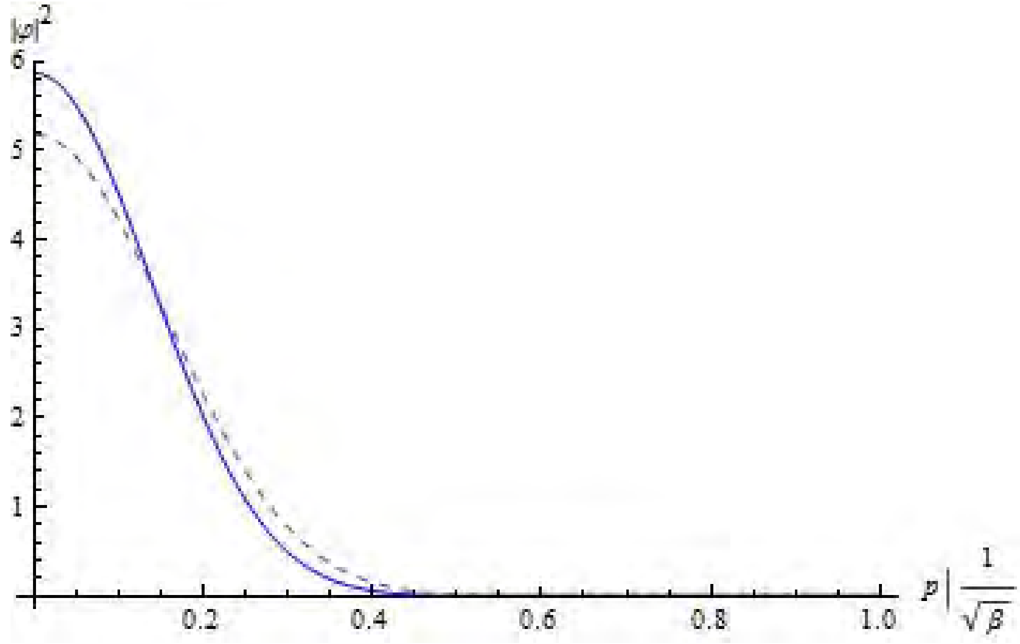

Figure 4.2: Probability density in the momentum space for $\frac{1}{2\beta\lambda} = 30$ and m=59 for n=2(solid line) and n=20(dotted line)

Recall that in attempting to solve the problem, a transformation of p into the complex plane p' is done. We have introduced a non-hermitian 'Hamiltonian' in Eqn.(4.29). This is reflected by the complex potential[19]. However, we would like to obtain the solution of the observable Hamiltonian as this is what we will be observing in experiments. Simultaneously, we are able to investigate the effects of the complex potential of our problem, that is, the role of the imaginary part of the potential.

To obtain the observable solution and investigate the effects of the complex potential, we begin with Eqn.(4.29) and dropping the imaginary part of the potential. This ensures that the Hamiltonian is hermitian and correspond to an observable quantity; the energy eigenvalue in this case. We then obtain the following from Eqn.(4.29),

[19] Non-Hermitian Quantum Mechanics(NHQM) is not studied in-depth as it consists of new interpretations/effects to the Hermitian Quantum Mechanics. NHQM is mentioned here is to provide a supporting evidence to the existence of the solutions obtained above, that a solution can be obtained from a non-hermitian Hamiltonian.

$$\left[-\frac{d^2}{dx^2} + \mu' sech^2 x\right] \varphi_m^{(j)} = k^2 \varphi_m^{(j)} \tag{4.53}$$

where

$$\mu' = \frac{1}{\beta\lambda}(m'_j \pm 1 + \lambda\beta(\mp m'_j - \frac{1}{2})) + \frac{1}{4} - m'^2_j - \frac{1}{2\beta^2\lambda^2} \tag{4.54}$$

and k has the same definition as before. It is clear that this is again a Schrodinger-like equation[20] with potential of the form in Eqn.(4.34) with b=0. Hence,

$$-a^2 - a = \mu' = \frac{1}{\beta\lambda}(m'_j \pm 1 + \lambda\beta(\mp m'_j - \frac{1}{2})) + \frac{1}{4} - m'^2_j - \frac{1}{2\beta^2\lambda^2}. \tag{4.55}$$

For j=1,

$$a_1 = -\frac{1}{2} - \alpha_1 \tag{4.56}$$

$$a_1 = -\frac{1}{2} + \alpha_1 \tag{4.57}$$

where

$$\alpha_1 = \frac{1}{\sqrt{2}\beta\lambda}\sqrt{(\beta\lambda(m+1)-1)^2 + m^2\beta^2\lambda^2} \tag{4.58}$$

while for j=2,

$$a_2 = -\frac{1}{2} - \alpha_2 \tag{4.59}$$

$$a_2 = -\frac{1}{2} + \alpha_2 \tag{4.60}$$

where

[20] Recall that the m'_j has the same definition as above

$$\alpha_2 = \frac{1}{\sqrt{2}\beta\lambda}\sqrt{(m\beta\lambda - 1)^2 + ((m+1)\beta\lambda)^2}. \tag{4.61}$$

The above values of a_j is then subjected to the same constraints/range $-\frac{1}{2} < a_j \leq \frac{1}{2\beta\lambda}$, which then results in the following energy spectrum. The energy spectrum is arranged according to the values of m and the states are build with the same energy eigenvalues. Similarly, the negative energy eigenvalues can be obtained through Eqn.(4.38).

After dropping the imaginary part of the potential, it is observed that the four distinct bands of the energy spectrum combined into one band and is of a finite range. Once again, we see that there is an upper bound to the bound states. The uppermost bound state is denoted by $n_{max} < a_j$. In addition, the same characteristic extension of the energy spectrum to infinitely wide band (that is, the widening range of values of m to the whole real line) and the infinite number of bound states in the limit of $\beta \to 0$ is observed.

$E_{m,n} = \sqrt{M^2c^4 + c^2\left(\frac{1}{\beta} - 4\beta\lambda^2(-\frac{1}{2} + \alpha_1 - n)^2\right)}$		$n = 0, 1, 2, ... < a_1$
$\psi_{m,n}(p) = \begin{pmatrix} \psi^{(1)}_{m,n}(p) \\ 0 \end{pmatrix}$	$\psi^{(1)}_{m,n}(p) = p^{-\frac{1}{2}}(\frac{1}{1-\beta p^2})^{-\frac{a_1}{2}} R_n^{(a_1+\frac{1}{2},0)}(\frac{\sqrt{\beta}p}{\sqrt{1-\beta p^2}})e^{im\theta}$,	$a_1 = -\frac{1}{2} + \alpha_1$

Table 4.4: Energy levels and the corresponding wavefunctions for $m_- \leq m \leq m_+$, where $m_\pm = \frac{1-\beta\lambda}{2\beta\lambda} \pm \frac{1}{2\beta^2\lambda}\sqrt{\beta(1+\beta(4\beta\lambda - 1))}$.

$E_{m,n} = \sqrt{M^2c^4 + c^2\left(\frac{1}{\beta} - 4\beta\lambda^2(-\frac{1}{2} + \alpha_2 - n)^2\right)}$		$n = 0, 1, 2, ... < a_2$
$\psi_{m,n}(p) = \begin{pmatrix} 0 \\ \psi^{(2)}_{m,n}(p) \end{pmatrix}$	$\psi^{(2)}_{m,n}(p) = p^{-\frac{1}{2}}(\frac{1}{1-\beta p^2})^{-\frac{a_2}{2}} R_n^{(a_2+\frac{1}{2},0)}(\frac{\sqrt{\beta}p}{\sqrt{1-\beta p^2}})e^{i(m+1)\theta}$,	$a_2 = -\frac{1}{2} + \alpha_2$

Table 4.5: Energy levels and the corresponding wavefunctions for $m = \frac{1}{2\beta\lambda}(1 - \beta\lambda)$.

In table 4.4 and 4.5, it is noted that most of the states are spin singlet unless the value of β and λ results in $m = \frac{1}{2\beta\lambda}(1-\beta\lambda)$ to be an integer. Since only in this case, a spin down state is possible and the spinor components can have same energy eigenvalues for certain states. In the limit of $\beta \to 0$, apart from the widening of the band in table 4.4, the states in table 4.5 will exist for all values of m as seen from the inequalities of a_j that arise from the constraints. However, for a finite value of β, the states will only exist for specific value of m.

The behaviour of the wavefunctions is also investigated as n increases. Following the previous discussion, the probability density can be plotted in the x-domain.

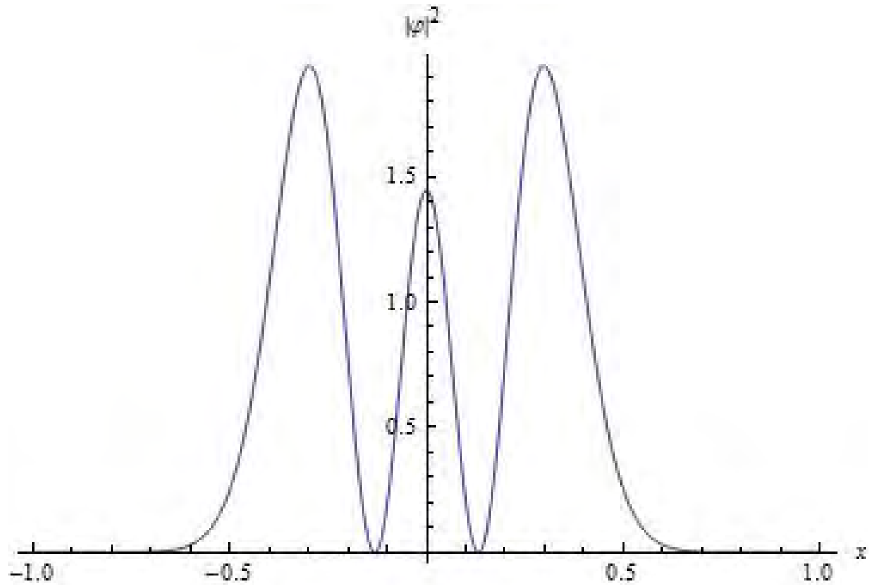

Figure 4.3: Probability density in the x-domain for $\lambda = 1$, $\beta = 0.1$, m=38, n=2.

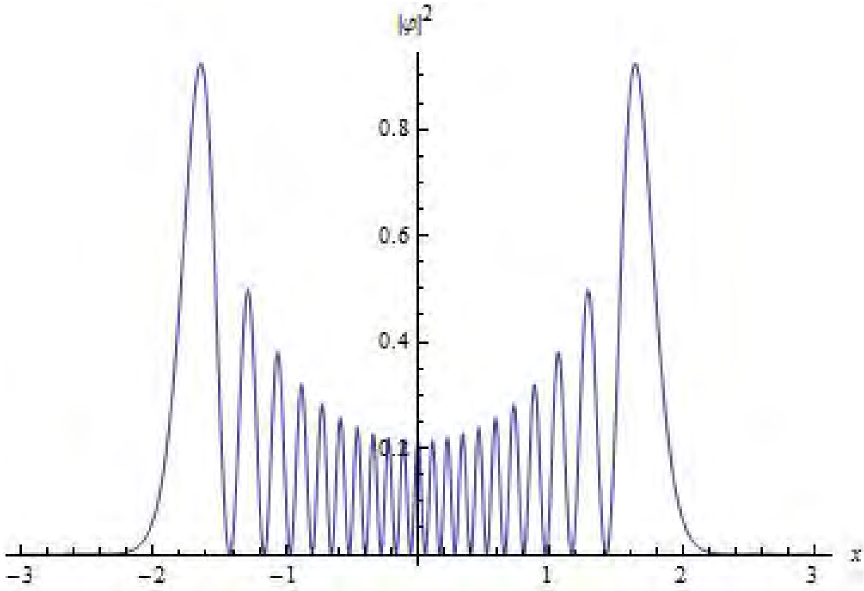

Figure 4.4: Probability density in the x-domain for $\lambda = 1$, $\beta = 0.1$, m=38, n=20.

From the two graphs, it is observed that as n increases, the dominant peak shifts away from the origin. This shows that as n increases, there is a higher probability in finding the particle at larger x (smaller x, for the negative region), both a correspondingly higher momentum. It is also observed that as n increases, more peaks appear and the ratio of the dominant peak to the lowest peak increases. This is in contrast to the previous case where in figure 4.1, we see that even as n increases, the probability density remains as a Gaussian distribution. Hence, we can deduce that with a complex potential, the imaginary part play a role in restraining the behaviour of the wavefunctions. This is reflected by the probability density having only a gradual change over n.

We shall now look at the undeformed case as a contrasting case. Starting from Eqn.(4.24) and setting $\beta = 0$, we have

$$\left(\frac{d^2}{dp^2} + \frac{1}{p^2}\left(\frac{1}{4} - m_j'^2\right) + \frac{\varepsilon^2}{\lambda^2} - \frac{2}{\lambda}(m_j' \pm 1) - \frac{p^2}{\lambda^2}\right)\varphi_m^{(j)}(p) = 0. \tag{4.62}$$

We will solve the above equation by exploiting the asymptotic analysis of the dominant behaviour at the end points. This method is similar to the one of the employed in solving the harmonic oscillator or hydrogen atom. Here we obtain

$$\varphi_m^{(j)}(p) = p^{\frac{1}{4}(2\mp 4m'_j)} f^{(j)}(p) e^{-\frac{p^2}{2\lambda}} \tag{4.63}$$

where "-" is assumed for $m'_j < \frac{1}{2}$ and "+" for $m'_j > -\frac{1}{2}$ and m'_j=m or m+1 for j=1,2 respectively. And $f^{(j)}(p)$ satisfies the following equation, considering $m'_j < \frac{1}{2}$,

$$\left(\frac{d^2}{dp^2} + \left[\frac{1-2m'_j}{p} - \frac{2p}{\lambda}\right]\frac{d}{dp} + \frac{\varepsilon^2}{\lambda^2} - \frac{2}{\lambda}(1\pm 1)\right) f^{(j)}(p) = 0. \tag{4.64}$$

Let $\chi = \frac{p^2}{\lambda}$, then

$$\left(\chi\frac{d^2}{d\chi^2} + \left[1 - \frac{1}{2}m'_j - \chi\right]\frac{d}{d\chi} + \frac{\varepsilon^2}{4\lambda} - \frac{1}{2}(1\pm 1)\right) f^{(j)}(\chi) = 0. \tag{4.65}$$

By assuming that $f(\chi)$ can be written as a power series $f^{(j)}(\chi) = \sum c_k \chi^k$, one notes that a truncation in the number of terms have to be effected; otherwise it leads to unnormalizable solution. This truncation condition leads to the quantization

$$\frac{\varepsilon^2}{2\lambda} - (1\pm 1) = n, \qquad \text{where n=0,1,2,..} \tag{4.66}$$

$$E^2 = M^2c^4 + 2\lambda c^2(n + (1\pm 1)). \tag{4.67}$$

The same argument holds for $m'_j > -\frac{1}{2}$, obtaining the same energy eigenvalues as above. The solutions for the Eqn.(4.65) is given by the associated Laguerre polynomials. Hence, the wavefunctions are given by

$$\psi_{m,n}^{(j)}(p) = p^{\mp m'_j} e^{-\frac{p^2}{2\lambda}} L_n^{\mp\frac{1}{2}m'_j}\left(\frac{p^2}{\lambda}\right). \tag{4.68}$$

In the undeformed case, it is observed that the energy spectrum has two distinct bands($m'_j < \frac{1}{2}$ and $m'_j > -\frac{1}{2}$). We shall take a look at the behaviour of the wavefunctions as n increases and compare it with that of the deformed problem.

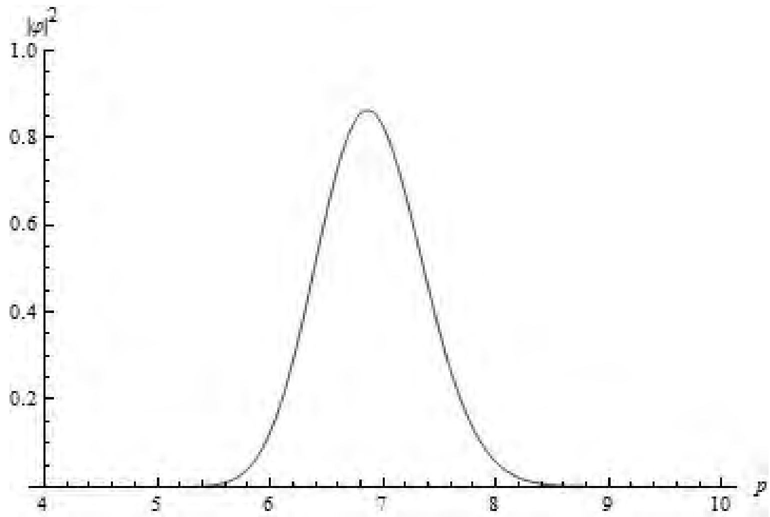

(a) zoom out view for the whole range

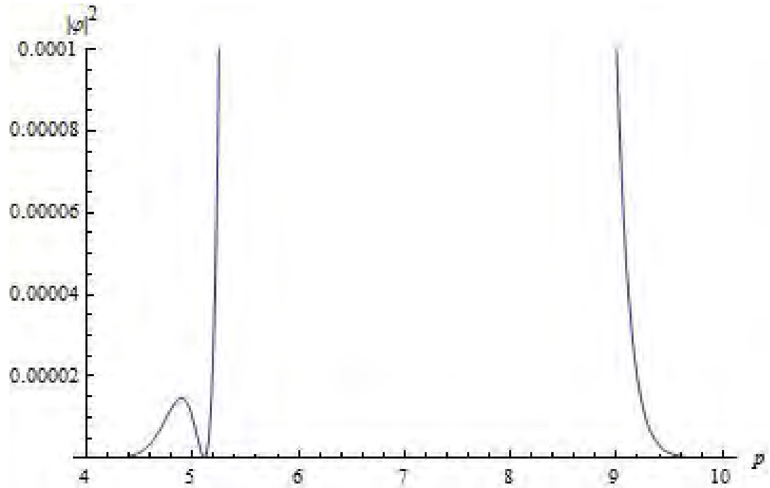

(b) zoom in view on small features

Figure 4.5: Probability density in momentum space for m=38, n=2

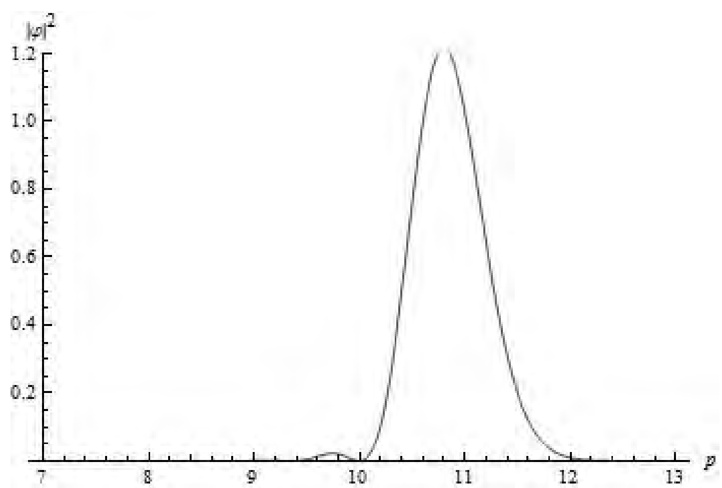

(a) zoom out view for the whole range

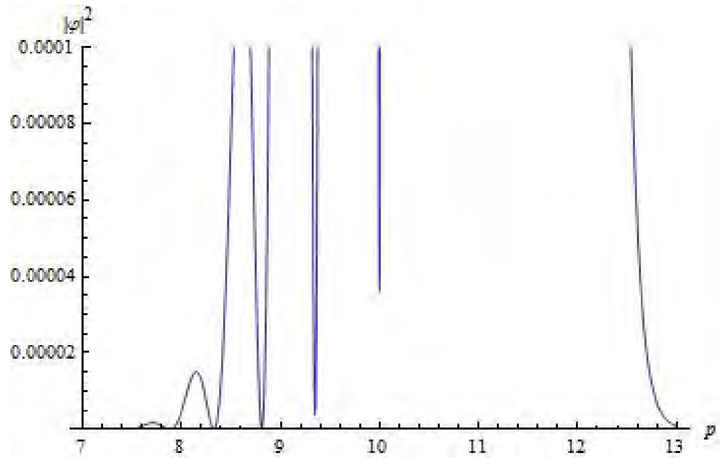

(b) zoom in view on small features

Figure 4.6: Probability density in momentum space for m=38, n=20

In contrast to figure 4.2, it is observed that the undeformed case has probability density in which its peak shift towards higher momentum values with increasing n. In addition, as n increases, more peaks appear. It is interesting to note that such behaviour can also be observed with the solutions of Eqn.(4.53) as shown in the following graphs.

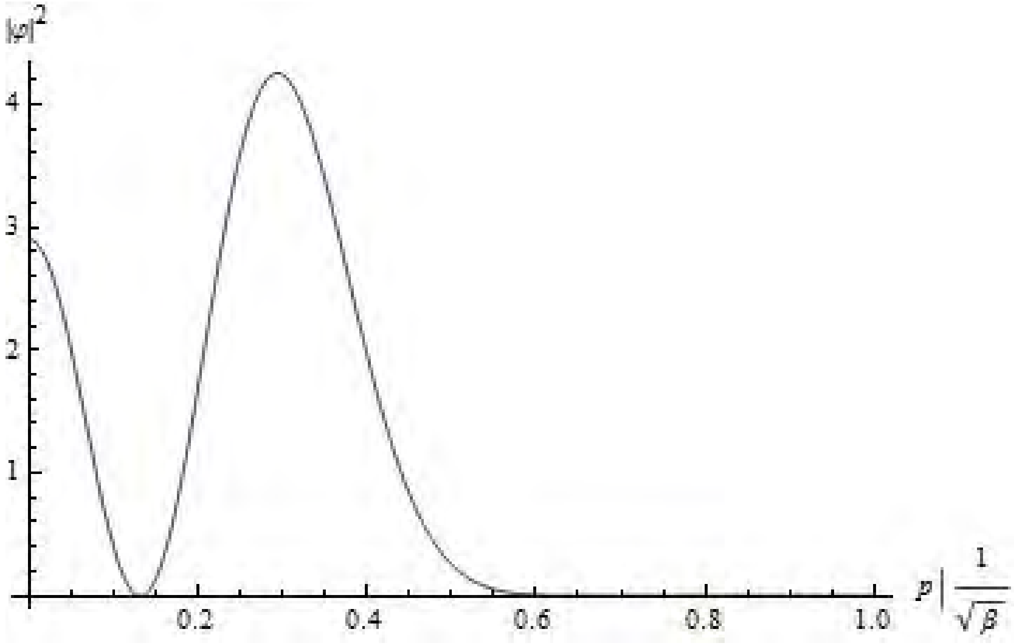

Figure 4.7: Probability density in momentum space for $\beta = 0.1$, $\lambda = 1$, m=38, n=2

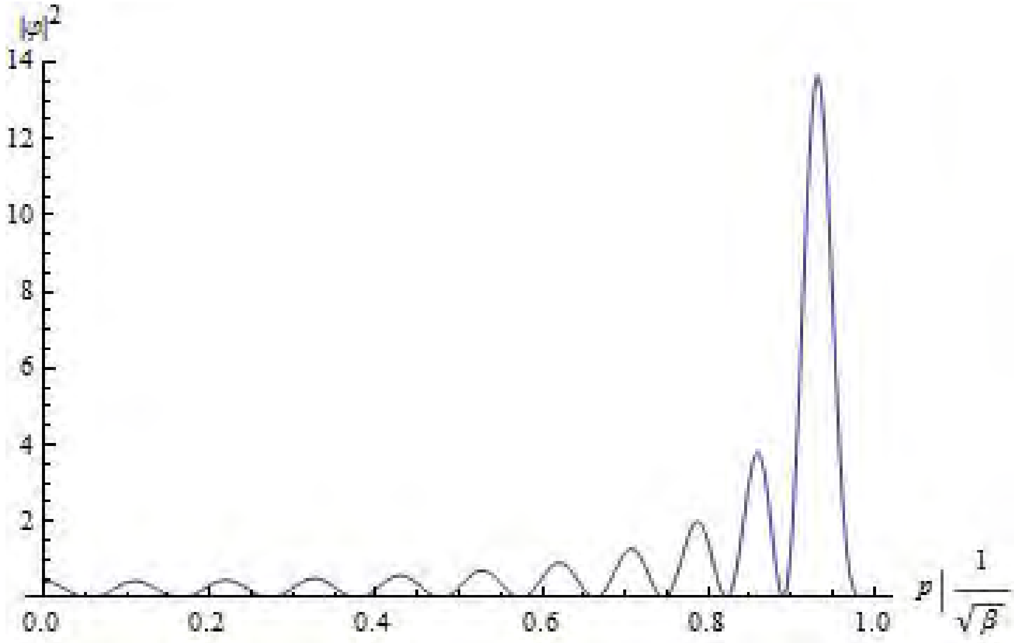

Figure 4.8: Probability density in momentum space for $\beta = 0.1$, $\lambda = 1$, m=38, n=20

From the similar behaviour, we deduce that the complex potential does have a restraining effect on the behaviour of the wavefunction. Here, we do not observe the same shifting of dominant peak towards the higher momentum(in the deformed case, the maximum momentum).

4.5 Massless Dirac equation in (2+1) dimensions

The Hamiltonian for the electrons in graphene in the presence of magnetic field is similar to the (2+1) dimensional massless Dirac equation with Fermi velocity v_F,

$$H_{massless} = c\sigma \cdot (\mathbf{P} + \frac{e}{c}\mathbf{A}) \rightarrow H_{graphene} = v_F\sigma \cdot (\mathbf{P} + \frac{e}{c}\mathbf{A}) \tag{4.69}$$

Following the above discussion, to solve this problem, only a minor change is required, which is

$$\varepsilon \rightarrow \varepsilon' = \frac{E}{v_F} \tag{4.70}$$

where $\varepsilon = E/c$. This means that the above discussions are similar except a minor change to the energy levels, which becomes

$$E_{m,n} = v_F\sqrt{\frac{1}{\beta} - 4\beta\lambda^2(a-n)^2} \tag{4.71}$$

Chapter 5

Energy Dispersion Relation

Apart from quantum mechanical implications, we see that MCRs have an implication on the energy dispersion relation as seen in Ref.[6]. We will now proceed to work out the modified dispersion relation under anti-Synder's algebra.

Recall that $[X_i, P_j] = i\hbar\delta_{ij}(1 - \beta P^2)$ where i,j=1,2,3. In the position representation, $X^i = x_0^i$ and $P^i = f(p_0^i)$, then[21]

$$
\begin{aligned}
< [X_i, f(P_0^j)] > &= i\hbar\delta_i^j < (1 - \beta f(P_0^k)^2) > \\
i\hbar\frac{\partial f(p_0^i)}{\partial p_0^i} &= i\hbar(1 - \beta f(p_0^i)^2) \\
\frac{\partial f(p_0^i)}{1 - \beta f(p_0^i)^2} &= \partial p_0^i \\
P^i = f(p_0^i) &= \frac{1}{\sqrt{\beta}}\tanh(\sqrt{\beta}p_0^i). \qquad (5.1)
\end{aligned}
$$

[21] X_0^i and P_0^i are the usual low energy operators that satisfy Heisenberg algebra. $P^i = f(P_0^i)$ comes from the motivation to express P^i in terms of operators that are associated with the familiar Heisenberg algebra.

We now have

$$X^\mu = (ct, x_0^i) \tag{5.2}$$

$$P^\mu = (E/c, P^i = p_0^i \left(1 - \frac{\beta}{6}|p_0|^2\right)) \tag{5.3}$$

where P^μ is the 4-momentum and $\mu = 0, 1, 2, 3$. Here we have effected an expansion and kept terms up to $O(\beta)$. Under the general static metric $g_{\mu\nu}$, the norm of P^μ takes the form

$$\begin{aligned} P^\mu P_\mu = g_{\mu\nu} P^\mu P^\nu &= g_{00}(P^0)^2 + g_{ij} P^i P^j \\ &= g_{00}\frac{E^2}{c^2} + g_{ij} p_0^i p_0^j \left(1 - \frac{\beta}{6}|p_0|^2\right)^2 \\ &= g_{00}\frac{E^2}{c^2} + g_{ij} p_0^i p_0^j \left(1 - \frac{\beta}{3}|p_0|^2\right). \end{aligned} \tag{5.4}$$

We recognize that under a general static metric, $g_{00}\frac{E^2}{c^2} + g_{ij} p_0^i p_0^j$ is a scalar of the undeformed norm. We denote this by γ. Hence, in terms of low momentum p_0^i,

$$P^\mu P_\mu = \gamma - g_{ij} p_0^i p_0^j \frac{\beta}{3}|p_0|^2. \tag{5.5}$$

We can rewrite the above in terms of high momentum by finding p_0^i in terms of P^i. This is shown below, up to $O(\beta)$

$$\begin{aligned} p_0^i &= \frac{1}{\sqrt{\beta}} \tanh^{-1}(\sqrt{\beta} P^i) \\ &\approx P^i \left(1 + \frac{\beta}{3}|P|^2\right). \end{aligned}$$

Eqn.(5.5) can then be written as

$$P^\mu P_\mu = \gamma - g_{ij} P^i P^j \frac{\beta}{3}|P|^2 \tag{5.6}$$

where we have kept terms up to $O(\beta)$. Recall that $P^\mu P_\mu = g_{00}(P^0)^2 +$

$g_{ij}P^iP^j$, then

$$(P^0)^2 = -\frac{1}{g_{00}}\left(-\gamma + g_{ij}P^iP^j\left(1+\frac{\beta}{3}|P|^2\right)\right). \tag{5.7}$$

The energy of a particle in static gravitational field $g_{\mu\nu}$ is given by

$$E^2 = (-g_{00}cP^0)^2 = -g_{00}c^2\left(-\gamma + g_{ij}P^iP^j\left(1+\frac{\beta}{3}|P|^2\right)\right). \tag{5.8}$$

We now see that in the Minkowski spacetime where $g_{00} = -1$, $\gamma = -m^2c^2$. Hence, we arrived at the modified energy dispersion relation

$$\begin{aligned} E^2 &= c^2\left(m^2c^2 + |P|^2\left(1+\frac{\beta}{3}|P|^2\right)\right) \\ &= E_0^2 + \frac{\beta}{3}|P|^4c^2 \end{aligned} \tag{5.9}$$

where $E_0^2 = m^2c^4 + |P|^2c^2$, the usual relativistic energy dispersion relation.

5.1 Application to Neutrino Physics

The modified energy dispersion relation can be applied to neutrino physics to obtain a bound on the deformation parameter β through experimental measurements.

Before we start, we will give a brief introduction to neutrino oscillation. Neutrino oscillations refer to the physics of neutrino flavour change. It is used to explain the solar neutrino problem [9] - the number measured fall short of the expected value[22].

Here we will only consider the case of two neutrino types, electron and muon neutrino. As mentioned in Ref.[6], we see that the neutrino is

[22] The measurement yield only a third of what is expected.

not an eigenfunction of the Hamiltonian since it can change into another type. Hence, we would expect that the eigenstates are orthogonal linear combinations:

$$\nu_1 = \nu_\mu \cos\theta - \nu_e \sin\theta \tag{5.10}$$

$$\nu_2 = \nu_\mu \sin\theta + \nu_e \cos\theta \tag{5.11}$$

where the coefficients are chosen for a normalized states and θ is the mixing angle. These states will then evolve through time with a phase factor as

$$\nu_1(t) = \nu_1(0)e^{-i\frac{E_1}{\hbar}t} \tag{5.12}$$

$$\nu_2(t) = \nu_2(0)e^{-i\frac{E_2}{\hbar}t}. \tag{5.13}$$

Now, we suppose that the particle is an electron neutrino at t=0, then from Eqn.(5.10) and Eqn.(5.11),

$$\nu_1(0) = -\sin\theta \tag{5.14}$$

$$\nu_2(0) = \cos\theta. \tag{5.15}$$

We can solve Eqn.(5.10) and Eqn.(5.11) for ν_μ and using the above,

$$\begin{aligned}\nu_\mu(t) &= \nu_1(t)\cos\theta + \nu_2(t)\sin\theta \\ &= \sin\theta\cos\theta\left(-e^{-i\frac{E_1}{\hbar}t} + e^{-i\frac{E_2}{\hbar}t}\right).\end{aligned} \tag{5.16}$$

The probability of electron neutrino converting into muon neutrino after time t is given by

$$\begin{aligned}P_{\nu_e\to\nu_\mu} = |\nu_\mu(t)|^2 &= (\sin\theta\cos\theta)^2\left(-e^{-i\frac{E_1}{\hbar}t} + e^{-i\frac{E_2}{\hbar}t}\right)^2 \\ &= \left(\sin(2\theta)\sin\left(\frac{E_2 - E_1}{2\hbar}t\right)\right)^2\end{aligned} \tag{5.17}$$

$$P_{\nu_e \to \nu_\mu} = \left(\sin(2\theta) \sin\left(\frac{(m_2^2 - m_1^2)c^4}{4\hbar E} t \right) \right)^2 \tag{5.18}$$

where E_1 and E_2 are the usual relativistic energy relations and we have assumed $E \approx |P|c$ and they have the same $|P|$. The above shows that the neutrino flavour will oscillate between electron and muon neutrino. We can see that if there is no mixing, the probability above will be zero immediately. Similarly, if the neutrinos are massless then $m_2^2 - m_1^2 = 0$, neutrino flavour change is also not possible. This shows the condition for neutrino oscillation. In experiments, the value of $m_2^2 - m_1^2$ can then be determined.

At this stage, we are in position to apply the modified energy dispersion relation (Eqn.(5.9)) to neutrino physics. In Eqn.(5.17), it depends on the energy difference between the two eigenstates. We can get the energy of each eigenstate from Eqn.(5.9),

$$\begin{aligned} E &= \sqrt{m^2c^4 + |P|^2c^2\left(1 + \frac{\beta}{3}|P|^2\right)} \\ &\approx |P|c\left(1 + \frac{1}{2}\left(\frac{m^2c^2}{|P|^2} + \frac{\beta}{3}|P|^2\right) - \frac{1}{4}\left(\frac{m^4c^4}{|P|^4} + \frac{2\beta}{3}m^2c^2\right)\right) \\ &\approx |P|c\left(1 + \frac{1}{2}\left(\frac{m^2c^2}{|P|^2} + \frac{\beta}{3}|P|^2\right)\right). \end{aligned} \tag{5.19}$$

In obtaining the above, we have made several assumptions. Firstly, $m^2c^2 << |P|^2$ and keeping up to second order approximation. In addition, we also kept terms of order β. Secondly, we have assumed that $\frac{m^2c^2}{|P|^2}$ and $\frac{\beta}{3}|P|^2$ has the same order. Hence, in keeping to first order approximation, we arrived at the last line of the above equation.

We can now insert Eqn.(5.19) into Eqn.(5.17) and assuming that they have the same $|P|$ and $|P|c \approx E$ as mentioned in Ref.[9].

$$\begin{aligned}
P_{\nu_e \to \nu_\mu} &= \left(\sin(2\theta) \sin\left(\frac{E_2 - E_1}{2\hbar} t \right) \right)^2 \\
&= \left(\sin(2\theta) \sin\left(\frac{|P|c \left(\left(\frac{(m_2^2 - m_1^2)c^2}{|P|^2} + \frac{\beta_2 - \beta_1}{3} |P|^2 \right) \right)}{4\hbar} t \right) \right)^2 \\
&\approx \left(\sin(2\theta) \sin\left[\left(\frac{(m_2^2 - m_1^2)c^4}{4\hbar E} + \frac{(\beta_2 - \beta_1)E^3}{12\hbar c^2} \right) t \right] \right)^2 . \qquad (5.20)
\end{aligned}$$

This is the probability/neutrino oscillation under the modified dispersion relation. From Eqn.(5.20), we see that there are two cases in which neutrino oscillation is possible. First, for massless or degenerate mass neutrinos, the neutrino oscillation is possible by the difference in the deformation parameters β_1 and β_2 as seen by each of the eigenstates. In this case, the term $\frac{(\beta_2 - \beta_1)E^3}{12\hbar c^2}$, corresponding to $\frac{((m_2^2 - m_1^2)c^4)}{4\hbar E}$ in the original case, is responsible for the neutrino oscillation. Thus,

$$\begin{aligned}
\frac{(m_2^2 - m_1^2)c^4}{4\hbar E} &= \frac{(\beta_2 - \beta_1)E^3}{12\hbar c^2} \\
\beta_2 - \beta_1 &= \frac{3(m_2^2 - m_1^2)c^6}{E^4} . \qquad (5.21)
\end{aligned}$$

Experimentally, $m_2^2 - m_1^2 = 8.0 * 10^{-5} eV^2$ and E=1 GeV as mentioned by [10]. Using this values, then we see that $\beta_2 - \beta_1$ (in $(kg^{-2}m^{-2}s^2)$) is of the order 10^{-23}.

Secondly, if the deformation parameters are constant, neutrino oscillation will be possible by difference in masses since Eqn.(5.20) has the same form as Eqn.(5.17) up to the first order approximation. We see that Eqn.(5.19) does contain higher order terms involving the deformation parameter. The next leading order correction will then turn up as the uncertainty in the experimental measurements. This then allow us to work out the bound on the deformation parameter, which can be done by demanding that this leading correction is smaller than the experimental uncertainty.

Chapter 6

Future Direction

We have seen that the relativistic landau problem under Synder's and anti-Synder's algebra lead to different results. One result is the modified energy spectrum. Under Synder's algebra, there is an additional spectrum that does not exist in the usual problem. On the other hand, under the anti-Synder's algebra, similar appearance of additional spectrum is observed with the non-hermitian Hamiltonian. In the latter case, a constrained spectrum is observed by demanding a hermitian Hamiltonian. Furthermore, under anti-Synder's algebra, there is an existence of an upper bound state. Such a modified energy spectrum along with its characteristics has not been studied in literature. The possible uses of these spectrum are unclear. What is interesting, however, is that such energy spectrum can be extended to graphene and hence, the study of these energy spectrum may lead to more potential uses of graphene.

Secondly, many MCRs have been proposed to introduce the idea of minimum length and maximum momentum into quantum mechanics. These MCRs would lead to different results of the same problem even though the deformation parameters are typically small. Hence, it is conceivable that in time to come, experiment can be used to determine the value of deformation parameter. In this way, we can then also compare the different MCRs to check which agrees best with experiment. Furthermore, the MCR that best agrees with experiment will indicate whether minimum length or maximum momentum or both exist.

Lastly, in the application of MCR to neutrino physics, the deformation parameter is seen to be of the order 10^{-23}. Here we have shown that, apart from mass differences, neutrino oscillations may also be accounted for by the deformation parameters. It would be interesting to investigate this possibility in the context of experimental work. In addition, we have only considered two types of neutrinos. We can extend this analysis to oscillations involving more neutrino flavours.

Chapter 7

Conclusion

Various quantum theories have predicted the existence of minimum length or maximum momentum. GUP has been developed in an attempt to study these effects in the context of quantum mechanics. In order to do this, the Heisenberg Uncertainty Principle has been modified by generalizing the right hand side of the underlying commutator relation. We have seen that different classes of MCRs, resulting from various constraints, do allow a minimum length; here interpreted as minimum uncertainty in position. Maximum momentum is also a feature of some of the theories. The latter is being introduced through a singularity in the weight function or the commutator relation.

We have also looked at various implications of MCR to quantum mechanics formalism. These include, among others, the introduction of the weight function in the completeness relationship, implying that the eigenfunctions are no longer orthonormal. In addition, the eigenstates may no longer be a physical state as seen in the case of relations that admit minimum length. Furthermore, several examples of deformed quantum mechanics from literature are discussed to show the different features that emerge under the conditions of minimum length and maximum momentum.

In the project, we have examined solutions to the relativistic Landau problem under the anti-Synder's algebra. In an attempt to solve the problem, we are forced to complexify the momentum. As a result, the Schrodinger-like equation consists of a complex potential. Here, by appealing to generalizations of the standard formalism of quantum mechanics (in the form of Non-Hermitian QM), we obtain solutions to this otherwise difficult problem. In this approach, the equation turns out to be exactly solvable. The resulting energy spectrum is shown to consists of an upper bound, which results from the finite orthogonality properties of the Romanovski polynomials. It is also observed that the energy spectrum results in four distinct bands, in which two bands have states that do not exist in the undeformed case. These states also vanishes in the $\beta \to 0$ limit, reducing them to the original state of the undeformed case. We have further examined the corresponding wavefunctions that are associated with these complex potential.

We have also applied the modified energy dispersion relation, arising from MCR, to neutrino physics. It is found that under the modified energy dispersion relation, neutrino oscillations are possible through two cases: difference in deformation parameters seen by each particle or difference in masses. In that section, we have also obtained an estimation of the deformation parameter as shown that it is of order 10^{-23}.

Acknowledgement

I would like to thank my supervisors A/P Kuldip Singh and Dr. Ng Wei Khim for devoting their time in guiding me along in this project. I also like to thank Ching Chee Leong for the helpful discussion.

Appendix A

G(P) in the proposed MCR

Substituting Eqn.(1.3) into Jacobi identity,

$$[F(P)\delta_{jk} + G(P)P_jP_k, X_i] - [F(P)\delta_{ik} + G(P)P_iP_k, X_j] = 0$$
$$[F(P), X_i]\delta_{jk} + [G(P)P_jP_k, X_i] - [F(P), X_j]\delta_{ik} - [G(P)P_iP_k, X_j] = 0.$$

From Eqn.(1.3), the operators in the momentum representation are

$$P_i = p_i, \qquad X_i = i\hbar\left(F(p)\frac{\partial}{\partial p_i} + G(p)p_ip_l\frac{\partial}{\partial p_l}\right). \tag{A.1}$$

Using these, the Jacobi identity becomes

$$[F(p), F(p)\frac{\partial}{\partial p_i} + G(p)p_ip_l\frac{\partial}{\partial p_l}]\delta_{jk} + [G(p)p_jp_k, F(p)\frac{\partial}{\partial p_i} + G(p)p_ip_l\frac{\partial}{\partial p_l}]$$
$$-[F(p), F(p)\frac{\partial}{\partial p_j} + G(p)p_jp_l\frac{\partial}{\partial p_l}]\delta_{ik} - [G(p)p_ip_k, F(p)\frac{\partial}{\partial p_j} + G(p)p_jp_l\frac{\partial}{\partial p_l}] = 0$$

$$
\begin{aligned}
[F(p)\frac{\partial F(p)}{\partial p_i} + G(p)p_ip_l\frac{\partial F(p)}{\partial p_l}]\delta_{jk} - [F(p)\frac{\partial F(p)}{\partial p_j} + G(p)p_jp_l\frac{\partial F(p)}{\partial p_l}]\delta_{ik} \\
+[F(p)\frac{\partial (G(p)p_jp_k)}{\partial p_i} + G(p)p_ip_l\frac{\partial (G(p)p_jp_k)}{\partial p_l}] \\
-[F(p)\frac{\partial (G(p)p_ip_k)}{\partial p_j} + G(p)p_jp_l\frac{\partial (G(p)p_ip_k)}{\partial p_l}] = 0.
\end{aligned}
\tag{A.2}
$$

We can make use of the fact that $p^2 = p_ip_i$, then $\frac{\partial p}{\partial p_i} = \frac{p_i}{p}$.

$$
\begin{aligned}
F(p)\frac{\partial F(p)}{\partial p}[\frac{p_i}{p}\delta_{jk} - \frac{p_j}{p}\delta_{ik}] + G(p)p\frac{\partial F(p)}{\partial p}[p_i\delta_{jk} - p_j\delta_{ik}] \\
+F(p)G(p)[p_j\delta_{ik} - p_i\delta_{jk}] = 0 \\
F(p)G(p) - G(p)p\frac{\partial F(p)}{\partial p} = F(p)\frac{\partial F(p)}{p\partial p}
\end{aligned}
$$

$$
G(p) = \frac{2F(p)\frac{dF(p)}{dp^2}}{F(p) - 2p^2\frac{dF(p)}{dp^2}}. \tag{A.3}
$$

This is the constraint that is shown in the thesis.

Appendix B

Wavefunction of 1D Harmonic Oscillator

After the change of variables, the equation becomes

$$\left[\xi^2\frac{\partial^2}{\partial\xi^2}+\xi\frac{\partial}{\partial\xi}-\frac{(1-\frac{\delta^2}{2}\xi)^2}{\delta^4}+\epsilon\right]\Psi(\xi)=0. \tag{B.1}$$

For $\xi \to 0$,

$$\left[\xi^2\frac{\partial^2}{\partial\xi^2}+\xi\frac{\partial}{\partial\xi}-k^2\right]\Psi(\xi)=0 \tag{B.2}$$

$$\left[\left(\xi\frac{\partial}{\partial\xi}\right)^2-k^2\right]\Psi(\xi)=0 \tag{B.3}$$

$$\left[\left(\xi\frac{\partial}{\partial\xi}-k\right)\left(\xi\frac{\partial}{\partial\xi}+k\right)\right]\Psi(\xi)=0 \tag{B.4}$$

where

$$k=\sqrt{\frac{1}{\delta^4}-\varepsilon}>0. \tag{B.5}$$

This gives

$$\Psi(\xi)=a\xi^k+b\xi^{-k} \tag{B.6}$$

where the term x^{-k} do not allow normalizability when $\xi \to 0$ and hence, not included. Thus, when $\xi \to 0$, $\Psi(\xi) \to \xi^k$.

On the other hand, for $\xi \to \infty$,

$$\left[\xi^2 \frac{\partial^2}{\partial \xi^2} + \xi \frac{\partial}{\partial \xi} - \frac{\xi^2}{4}\right] \Psi(\xi) = 0 \tag{B.7}$$

$$\left[\left(\xi \frac{\partial}{\partial \xi}\right)^2 - \frac{\xi^2}{4}\right] \Psi(\xi) = 0 \tag{B.8}$$

$$\left[\left(\xi \frac{\partial}{\partial \xi} - \frac{\xi}{2}\right)\left(\xi \frac{\partial}{\partial \xi} + \frac{\xi}{2}\right)\right] \Psi(\xi) = 0. \tag{B.9}$$

This gives

$$\Psi(\xi) = a e^{\xi/2} + b e^{-\xi/2}. \tag{B.10}$$

Similarly, $e^{\xi/2}$ do not allow normalizability when $\xi \to \infty$ and hence, not included. Thus, when $\xi \to \infty$, $\Psi(\xi) \to e^{-\xi/2}$.

This leads to the wavefunction to be

$$\Psi(\xi) = e^{-\xi/2} f(\xi) \, (\xi)^k \tag{B.11}$$

where $f(\xi)$ is the connection function of the asymptotic behaviour when ξ is not near the boundary.

Appendix C

Hypergeometric Equation

All classical orthogonal polynomials appear as solutions of the hypergeometric equation as shown below:

$$\sigma(x)y_n''(x) + \tau(x)y_n'(x) - \lambda_n y_n(x) = 0 \tag{C.1}$$

where

$$\sigma(x) = ax^2 + bx + c \tag{C.2}$$

$$\tau(x) = dx + e \tag{C.3}$$

$$\lambda_n = n(n-1)a + nd. \tag{C.4}$$

The solution denoted by

$$y_n(x) = P_n \left(\begin{array}{ccc|c} d & & e & \\ & & & \text{x} \\ a & b & c & \end{array} \right) \tag{C.5}$$

where a, b, c, d and e are the parameters of the polynomial and n (=0,1,2,...) is the order of the polynomial. The solution can be found using different methods [7]. The polynomials can be built from Rodrigues representation and are classified according to their weight functions $w(x)$ as shown below:

$$P_n = \frac{1}{W\left(\begin{matrix} d & & e \\ a & b & c \end{matrix}\middle| \text{x}\right)} * \frac{d^n}{dx^n}\left((ax^2+bx+c)^n W\left(\begin{matrix} d & & e \\ a & b & c \end{matrix}\middle| \text{x}\right)\right) \tag{C.6}$$

$$w(x) = W\left(\begin{matrix} d & & e \\ a & b & c \end{matrix}\middle| \text{x}\right) = exp\left(\int \frac{(d-2a)x+(e-b)}{ax^2+bx+c}dx\right). \tag{C.7}$$

For different parameters, the above solutions will yield the corresponding polynomials. For example, in Eqn.(3.10), the parameters correspond to that of Laguerre polynomial, a=0, b=1, c=0, d=-1 and e=2k+1. Hence, the solution to the equation is an associated Laguerre polynomial.

Appendix D

Romanovski Polynomial

Another set of parameters of the polynomial will be looked at since in this paper, the main solution consists of this class of polynomial: Romanovski polynomials. The corresponding set of parameters are a=1, b=0, c=1, d=2(1-p) and e=q where $p > 0$. Such a set of parameters results in the following weight function that belongs to this class of polynomial.

$$w(x) = (x^2 + 1)^{-p} e^{q \tan^{-1} x} \tag{D.1}$$

The orthogonality properties of the Romanovski polynomials are discussed in the main text. In Ref.[7] it is shown that Schrodinger equation with hyperbolic scarf potential(Eqn.(4.34)) reduces to the differential equation satisfied by the Romanovski polynomial. We shall discuss on the reason on the transformation of p to p'. Starting from the Schrodinger equation in Eqn.(4.26), a substitution of $x = \sinh q$ yield

$$\begin{aligned}(1+x^2)\frac{d^2\varphi_m^{(i)}(x)}{dx^2}+x\frac{d\varphi_m^{(i)}(x)}{dx}+\frac{1}{x^2(1+x^2)}\left[\left(\frac{1}{4}-m'^2\right)\right.\\ \left.-\frac{2x^2}{\beta\lambda}\left[(m'\pm 1)+\beta\lambda\left(\mp m'+\frac{1}{2}\right)\right]-\frac{x^4}{\beta^2\lambda^2}\right]\varphi_m^{(i)}(x)\\ +\frac{\varepsilon^2}{\beta\lambda^2}\varphi_m^{(i)}(x)=0.\end{aligned} \tag{D.2}$$

This equation is similar to the polynomial that has the weight function in Eqn.(D.1). Thus, it suggests the following substitution

$$\varphi_m^{(i)}(x)=(1+x^2)^{\frac{\mu}{2}}e^{-\frac{\nu}{2}\tan^{-1}x}D_n^{(\mu,\nu)(i)}(x), \tag{D.3}$$

obtaining

$$\begin{aligned}\left\{(1+x^2)\frac{d^2}{dx^2}+[(2\mu+1)x-\nu]\frac{d}{dx}\right.\\ +\frac{1}{x^2(1+x^2)}\left[\left(\frac{1}{4}-m'^2\right)+x^2\left(\frac{\nu}{2}+\frac{\nu^2}{4}+\mu-\mu^2\right.\right.\\ \left.\left.-\frac{2}{\beta\lambda}\left[(m'\pm 1)+\beta\lambda\left(\mp m'+\frac{1}{2}\right)\right]\right)+\mu\nu x^3-\frac{x^4}{\beta^2\lambda^2}\right]\\ \left.+\left(\mu^2+\frac{\varepsilon^2}{\beta\lambda^2}\right)\right\}D_n^{(\mu,\nu)(i)}(x)=0.\end{aligned} \tag{D.4}$$

The coefficient of the terms involving the factor $\frac{1}{x^2(1+x^2)}$ has to vanish, leading to

$$\frac{1}{\beta^2\lambda^2}=0. \tag{D.5}$$

This is approximately true only if $\beta,\lambda\to\infty$, which is not the case since in literature, β is a small value($<<1$). Recall also the definition of λ, B_0 has to be infinitely large in order for the above to hold approximately true. Hence, we see that by purely a change of variable to the q domain do not yield a solution, which in turn require us to perform a transformation of p to p'.

Appendix E

Dirac equation

Dirac equation is an equation for describing particles of spin $\frac{1}{2}$. It is a relativistic equation but is in contrast to the Klein-Gordon equation in which it is first order in time. Dirac' strategy [8] is to factorize the relativistic energy-momentum relation, which introduce the Dirac matrices in the process. Hence, the energy-momentum relation can be written as:

$$p^\mu p_\mu - m^2c^2 = (\gamma^k p_k + mc)(\gamma^\lambda p_\lambda - mc) = 0 \tag{E.1}$$

$$\gamma^0 = \begin{pmatrix} 1 & 0 \\ 0 & -1 \end{pmatrix} \qquad \gamma^i = \begin{pmatrix} 0 & \sigma^i \\ -\sigma^i & 0 \end{pmatrix} \tag{E.2}$$

where σ^i is the Pauli matrices. Thus, the Dirac equation by convention will be

$$i\hbar\gamma^\mu \partial_\mu \psi - mc\psi = 0, \quad \text{where} \quad \psi = \begin{pmatrix} \psi_1 \\ \psi_2 \\ \psi_3 \\ \psi_4 \end{pmatrix}. \tag{E.3}$$

The wavefunction now is a four-vector and is called the Dirac spinor.

References

[1] Chee Leong Ching, Rajesh R. Parwani, and Kuldip Singh, *Constraints and spectra of a deformed quantum mechanics*, Physical Review D 86, 084053(2012)

[2] Achim Kempf, Gianpiero Manganoy, and Robert B. Mannz, *Hibert Space Representation of the Minimal Length Uncertainty Relation*, Phys.Rev.D52:1108(1995)

[3] Chee Leong Ching, and Wei Khim Ng, *Generalization Relativistic Wave Equations with Intrinsic Maximum Momentum*, prepared of submission to JHEP

[4] Sabine Hossenfelder, *Minimal Length Scale Scenario for Quantum Gravity*, arVix:1203.6191v2[gr-qc](2013)

[5] Chee Leong Ching, and Rajesh R.Parwani, *Effect of Maximum Momentum on Quantum Mechanical Scattering and Bound States*, Modern Physics Letters A Vol. 28, No. 15 (2013) 1350061

[6] L.Menculini, O. Panella, and P. Roy, *Exact solutions of the (2+1) Dimensional Dirac equation in a constant magnetic field in the presence of a minimal length*, arVix:1302.4614v1 [hep-th](2013)

[7] D.E. Alvarez-Castillo, and M. Kirchbach, *Exact Spectrum and wave functions of the hyperbolic Scarf potential in terms of finite Romanovski polynomials*

[8] D. Griffiths, *Introduction to Elementary Particles*, Chapter 7: Quantum Electrodynamics, Wiley-VCH(2008)

[9] D. Griffiths, *Introduction to Elementary Particles*, Chapter 11: Neutrino Oscillations, Wiley-VCH(2008)

[10] Boris Kayser, *Neutrino Physics*,arXiv:hep-ph/0506165v1 (2005)